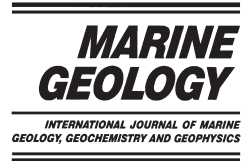




ELSEVIER

Marine Geology 181 (2002) 357–386



www.elsevier.com/locate/margeo

The effect of a submarine canyon on the river sediment dispersal and inner shelf sediment movements in southern Taiwan

James T. Liu*, Kuen-jang Liu, Jeff C. Huang

Institute of Marine Geology and Chemistry, National Sun Yat-sen University, Kaohsiung 804-24, Taiwan, ROC

Received 7 October 1999; accepted 3 July 2001

Abstract

This study examines the influence of a submarine canyon on the dispersal of sediments discharged by a nearby river and on the sediment movement on the inner shelf. The study area includes the head region of the Kao-ping Submarine Canyon whose landward terminus is located approximately 1 km seaward from the mouth of the Kao-ping River in southern Taiwan. Within the study area 143 surficial sediment samples were taken from the seafloor. Six hydrographic surveys along the axis of the submarine canyon were also conducted over the span of 1 yr. Three different approaches were used in the analysis of grain-size distribution pattern. They include (1) a combination of ‘filtering’ and the empirical orthogonal (eigen) function (EOF) analysis technique, (2) the McLaren Model, and (3) the ‘transport vector’ technique. The results of the three methods not only agree with one another, they also complement one another. This study reveals that the Kao-ping Submarine Canyon is relatively a stratified and statically stable environment. The hydrographic characteristics of the canyon display seasonal variability controlled primarily by the temperature field and the effluent of the Kao-ping River. The hydrographic condition and the bottom topography in the canyon suggest the propagation of internal tides during the flood season (summer) of the Kao-ping River. The submarine canyon acts as a trap and conduit for mud exchange between the Kao-ping River and offshore. Near the head of the canyon there is a region of sediment transport convergence. This region is also characterized by high mud abundance on the seafloor that coincides with the presence of high suspended sediment concentration (SSC) spots in the bottom nepheloid layer. Outside the submarine canyon on the shelf where the evidence of wave reworking is strong, the northwestward alongshore transport dominates over the southeastward transport, which is a common theme on the west coast in southern Taiwan. © 2002 Elsevier Science B.V. All rights reserved.

Keywords: Kao-ping Submarine Canyon; bottom nepheloid layer; mud trap; grain-size distribution; EOF analysis; McLaren Model; transport vector; static stability; internal tide

1. Introduction

Submarine canyons are common features on

continental margins worldwide (Baker and Hickey, 1986; Durrieu de Madron, 1994; Gardner, 1989; Hagen et al., 1996; Hickey et al., 1986). They are important natural conduits for the transfer of terrigenous sediments to the deep sea (Baker and Hickey, 1986; Carson et al., 1986;

* Corresponding author. Fax: +886-7-525-5130.

E-mail address: james@mail.nsysu.edu.tw (J.T. Liu).

Granata et al., 1999), and thus, preferential pathways for shelf–slope exchange (Durrieu de Madron, 1994). Submarine canyons are also loci of high suspended sediment concentrations and enhanced accumulation of modern sediment (Carson et al., 1986), and depocenters (Granata et al., 1999).

Submarine canyons are sometimes incorporated into a larger depositional system. On the southern coast of California, a type of repetitive coastal depositional systems has been identified as discrete sedimentation cells (Inman and Frautschy, 1966). Each cell contains a complete cycle of littoral transport and sedimentation, with rivers being the principal sources of sediments for the cells and the chief sinks being the submarine canyons which bisect the California continental shelf and intercept the sand as it moves along the beach (Inman and Frautschy, 1966). In such a system, there are a well-defined sediment source, a conduit, and a sink.

From a dynamics point of view, submarine canyons could be regions of enhanced mixing, and thus of enhanced exchange of properties between the shallow continental shelves and the deeper regions of the continental slope and rise (Hotchkiss and Wunsch, 1982). Important dynamic processes in canyons include internal waves, tides, quasi-geostrophic flows, turbidity currents, and storm-induced currents (Hotchkiss and Wunsch, 1982).

Sediment transport processes in submarine canyons are related to some of these processes. For example, at Baltimore Canyon, the sediment transport processes include resuspension events generated by tidal energy. The plume of turbid water then flows from the canyon along density surfaces (Gardner, 1989).

The topography of submarine canyons and coastal currents might interact to generate circulation through the canyon resulting in upwelling or downwelling near the canyon head (Freeland and Denman, 1982; Granata et al., 1999; Kinsella et al., 1987; Klink, 1996). When a submarine canyon is located near a river, the two systems often interact. In the case of Quinault Submarine Canyon, it intercepts the dispersal path of modern Columbia River sediments on the continental

shelf (Carson et al., 1986). In the case of Willapa Canyon, it becomes a site of preferential accumulation of Columbia River-derived particles (Baker, 1976). In the case of the littoral cells in southern California, the submarine canyon, the river, and the littoral system all have become an integral part of the coastal depositional system. Since rivers are major means for the introduction of terrestrial sediments into the coastal sea, and submarine canyons are conduits for the transfer of littoral sediments to the deep sea, it is of great scientific significance to examine how the two delivery systems relate and interact.

Therefore, the goal of this study is to examine how the existence of a submarine canyon affects the dispersal of river sediment and nearshore sediment transport from the perspective of grain-size distributions on the surface of the seafloor. Our particular attention is given to the head region of a submarine canyon located immediately seaward of the mouth of a river.

2. Study area

Submarine canyons have been documented for the waters around Taiwan (Yu et al., 1991, 1993; Yu and Hong, 1993; Yu and Wen, 1991). Our focus in this study is on the head region of the Kao-ping Submarine Canyon located in southern Taiwan. This submarine canyon extends almost immediately seaward from the mouth of the Kao-ping River down to the lower continental slope over a distance of 240 km (Fig. 1, (Yu et al., 1993). It eventually terminates in the northwestern corner of the South China Sea basin. This submarine canyon was considered the seaward continuation of the Kao-ping River (Yu et al., 1991). The head of the canyon, located about 1 km from the shoreline, is characterized by high and steep walls (Yu et al., 1993). The canyon has relief exceeding 600 m, whose cross-sectional geometry varies from V-shaped to broadly U-shaped (Yu et al., 1991). Some evidence from the canyon bottom topography suggests that the effect of deposition outweighs that of down-cutting (Yu et al., 1991). The origin and genesis of the canyon have been speculated to be related to

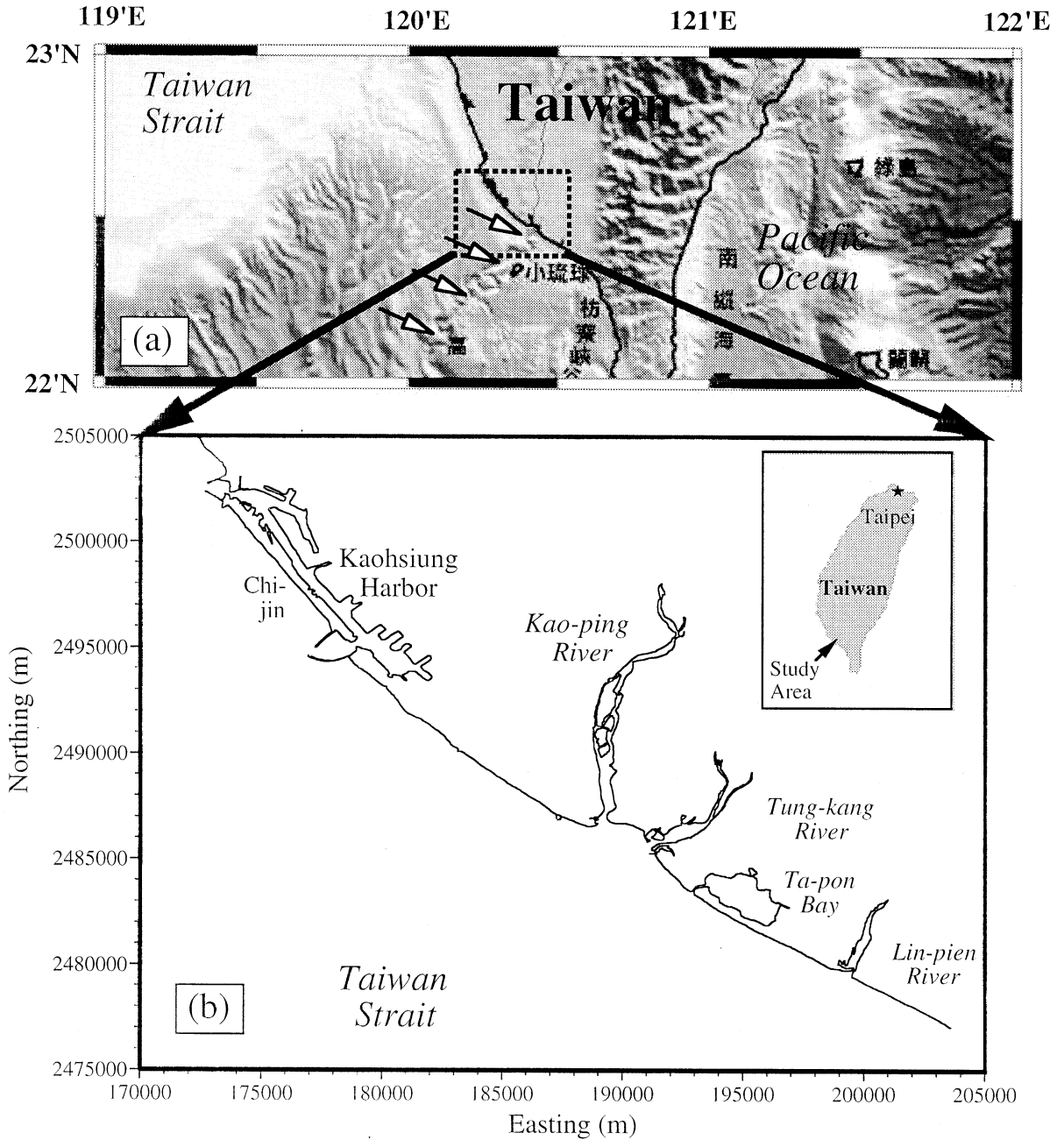


Fig. 1. (a) A schematic bathymetric relief map of the tip of southern Taiwan (provided by the National Center for Ocean Research). The arrows mark the location of the Kao-ping Submarine Canyon. The region indicated by the box of dashed lines is enlarged in (b) which shows the coastline of the study area including the confluence region of the Kao-ping River and Tung-kang River, Kaohsiung Harbor, and Chi-jin Barrier. The insert is a larger-scaled map of Taiwan.

subaerial erosion of the coastal plain at the last sea level low-stand, and submarine mass movements (Yu et al., 1991). However, a more recent study reveals that the formation of this submarine canyon is controlled by the tectonic evolution of the arc–continent collision between the Chinese continental margin and the Taiwan orogen. Consequently, many structural deformations in the Taiwan accretionary wedge were formed including the Kao-ping Submarine Canyon (Liu et al., 1997).

Within the canyon there is strong evidence indicating the existence of internal waves excited by tidal energy at the shelf edge (Wang and Chern, 1996). These internal waves are linked to the landward transport and coastal upwelling of colder water from the deeper part of the canyon. These internal waves could contribute to the transport of suspended sediments in the canyon. Wang and Chern (1996) also noticed that the surge of cold water at the head of the Kao-ping Submarine Canyon only occurred in late spring and summer. It was seldom observed in fall and winter. In a recent study, Wang et al. (2000) further reveal some unique properties of the internal tide inside the canyon. In the head region of the canyon the accumulation of coprostanol, which is a tracer for sewage pollution, suggests that the Kao-ping Submarine Canyon could be a trap for Kao-ping River sediments (Jeng et al., 1996).

The Kao-ping River is the largest river in Taiwan in terms of drainage area (3257 km²), the estimated mean annual runoff (8.46×10^9 m³), and the second largest in terms of suspended sediment discharge (3.6×10^7 MT) (Water Resources Bureau, 1998). Due to the influence of the monsoon, the annual discharge of the Kao-ping River concentrates in the summer season and early fall, culminating in August. On average, the amount of discharge in June, July, August, and September is equal to about 78% of the annual discharge of the river. The suspended sediment load estimated near the mouth of the river indicates that August also has the highest amount of suspended sediment discharge (Water Resources Bureau, 1998). The Tung-kang River is much smaller in terms of

the drainage area, runoff, and sediment discharge. Therefore, in this study, the influence of the Tung-kang River is ignored.

There is a common but unsubstantiated belief that most of the sediments discharged by the Kao-ping River will end up in the Kao-ping Submarine Canyon due to its closeness to the river mouth (Fig. 1). However, there is also indirect evidence indicating that the barrier/inlet system (Chi-jin/Kaohsiung Harbor) about 15 km north of the Kao-ping River mouth is likely a sediment sink for its fluvial sediments (Fig. 1). A study by Liu and Hou (1997) on the sediment trapping and by-passing characteristics around the north entrance of Kaohsiung Harbor shows that northward sediment longshore transport is the dominant mode of sediment movement off Chi-jin. The sediments on the beaches of Chi-jin are largely composed of fragments of metamorphic rocks of the Central Mountain Range of Taiwan, suggesting the Kao-ping River as the most likely source.

The wave field offshore of Chi-jin is closely coupled with the seasonal wind patterns (Wei et al., 1988). In the summer time, waves are influenced by southeasterly winds and typhoons, which are characterized as having longer and steeper waves (Wei et al., 1988). In the winter time, the wave field is dominated by northwesterly winds. However, the average wave height and wave period are smaller. The incident waves in both the summer and winter are more or less at a right angle to the Chi-jin shore, but the summer waves have more southerly components and the winter waves have more northerly components. The net littoral drift off Chi-jin is believed to be northward (Wei et al., 1990). Some year-round measurements of the flow field off the south entrance of Kaohsiung Harbor provided by the Institute of Harbor and Marine Technology indicate that the flows are predominantly longshore, having strong tidal periodicities. Tides in this area are probably of less importance with respect to coastal sediment dispersion. They are of mixed characteristics with semidiurnal tides dominating. The tidal range varies from 57 to 171 cm (Wei et al., 1990).

3. Data acquisition

3.1. Field work

3.1.1. Bathymetric survey

Two vessels were used in the bathymetric survey. Initially, a fishing boat was used for the survey between November 5 and 10, 1997 (Fig. 2). An integrated system for real-time positioning and water depth acquisition described by Liu et al. (2000) was employed in this operation. However, due to the frequency (200 Hz) of our echo sounder, the effective depth range was limited to 200 m. Consequently, no depth data were acquired over the region of submarine canyon proper where water depth exceeds 200 m.

In order to solve this problem, the R/V *Ocean Researcher III* was used, since her on-board echo sounder (Simrad EK500, 38 Hz) has a greater depth range. Subsequently, the second part of

this operation was conducted on November 17 and 18 to cover the area where data points were missing during the fishing boat survey (Fig. 2). Only the ship's GPS was used at this time, because of system incompatibility between our data acquisition system and the positioning system of the ship.

The raw bathymetric data from both parts of the survey were checked for spikes and then corrected for the tidal phase using tidal records (based on the Kee-lung mean sea level) provided by the Kaohsiung Harbor Bureau. Due to the NW–SE orientation of the survey transects, the coordinates of measured data positions (in easting and northing) were first transformed to shore-normal and shore-parallel coordinates and then gridded. The gridded data were contoured, which was subsequently merged with digitized coastline to render a detailed 2-D bathymetric map of the surveyed area.

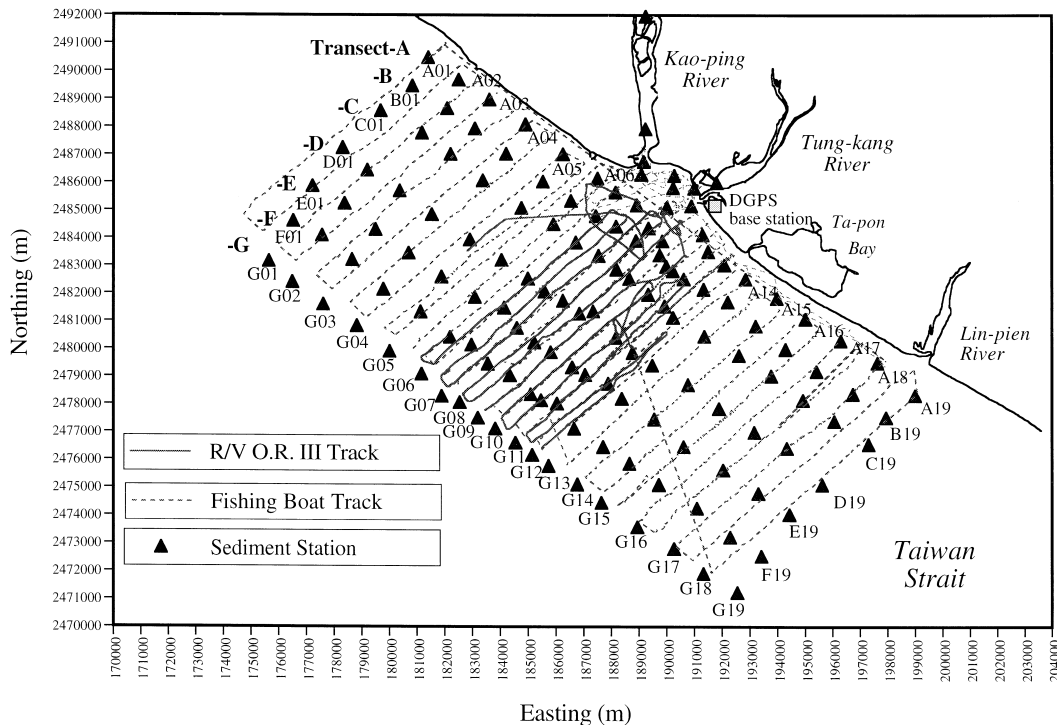


Fig. 2. The plot of all the bathymetric survey tracks (dashed and solid lines), sediment sampling stations (triangles). The seven shore-parallel sediment sampling transects are denoted by the alphabet from A to G. On each transect, sampling stations are numbered sequentially from 1 to 19. The location for the DGPS base station is represented by a square.

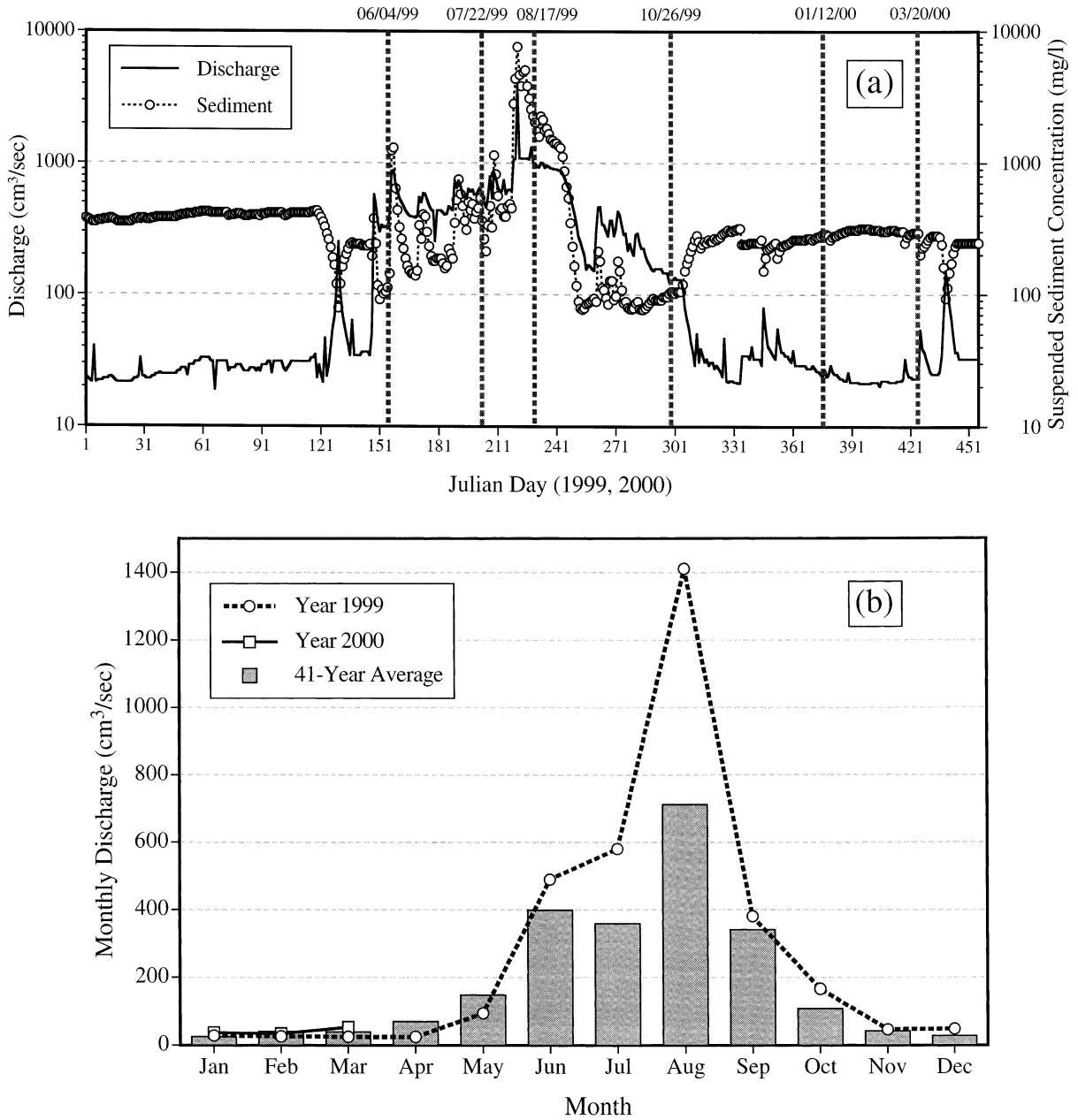


Fig. 3. (a) Daily river discharge and suspended sediment concentration measured at the nearest gauging station (approximately 34 km) to the river mouth from January 1, 1999 to April 30, 2000. Vertical dashed lines indicate the dates (listed above) at which six hydrographic surveys along the Kao-ping Submarine Canyon axis took place. The discharge and SSC data were provided by the Water Resources Bureau. (b) Monthly mean river discharge for the same period as (a) plotted over the mean discharge averaged over 41 years (1949–1990).

3.1.2. Sediment sampling and grain-size frequency analysis

From March to May, 1998, sediment samples from the surface of the seafloor in the study area were taken along seven shore-parallel transects (from A to G, Fig. 2) starting on the seaward side of the breaker point extending offshore, having spacings of about 1.2 km apart. There were 19 stations on each transect. Outside the submarine canyon region, the sampling intervals were approximately 0.8 km. Inside the submarine canyon area, the intervals were approximately 0.5 km.

Sampling along the innermost transect (A) was done using the same fishing boat with a custom-made grab sampler. Samples were also taken in the embayment area in which the mouths of both the Kao-ping River and Tung-kang River join,

and in the lower reaches of the Kao-ping River (Fig. 2). The R/V *Ocean Researcher III* was used for the rest of the sediment sampling using a Shipek grab sampler.

All the 143 sediment samples were processed and analyzed in a fashion similar to that described by Liu and Hou (1997) and Liu et al. (2000). Each sample was treated with 30% hydrogen peroxide solution to eliminate organic materials, and then wet-sieved to separate gravel (coarser than 2 μm , or -1ϕ), sand, and mud (finer than 0.063 μm , or 4ϕ). No gravel was recorded. The sand fraction was analyzed for grain-size frequency distribution using a custom-built rapid sediment analyzer (RSA), and recorded at quarter-phi intervals on a host personal computer. Twenty grain-size classes were registered (between 1.68 μm and 0.063 μm). The mud fraction was

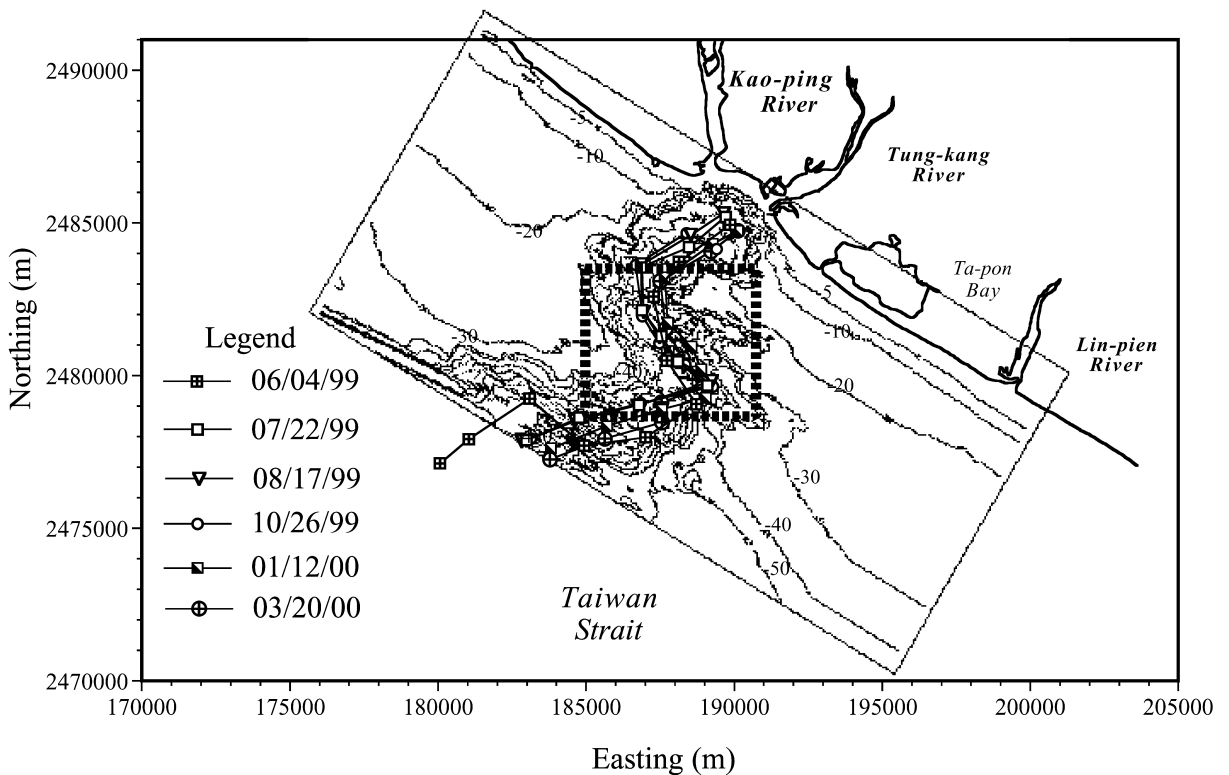


Fig. 4. The plot of the ship tracks for the six hydrographic surveys. The symbols indicate the positions of each profiling station. The bathymetric contour is in meters. The box of dashed lines indicates region of exceedingly high mud concentration on the surface of the seafloor, and high SSC in the lower water column (see text).

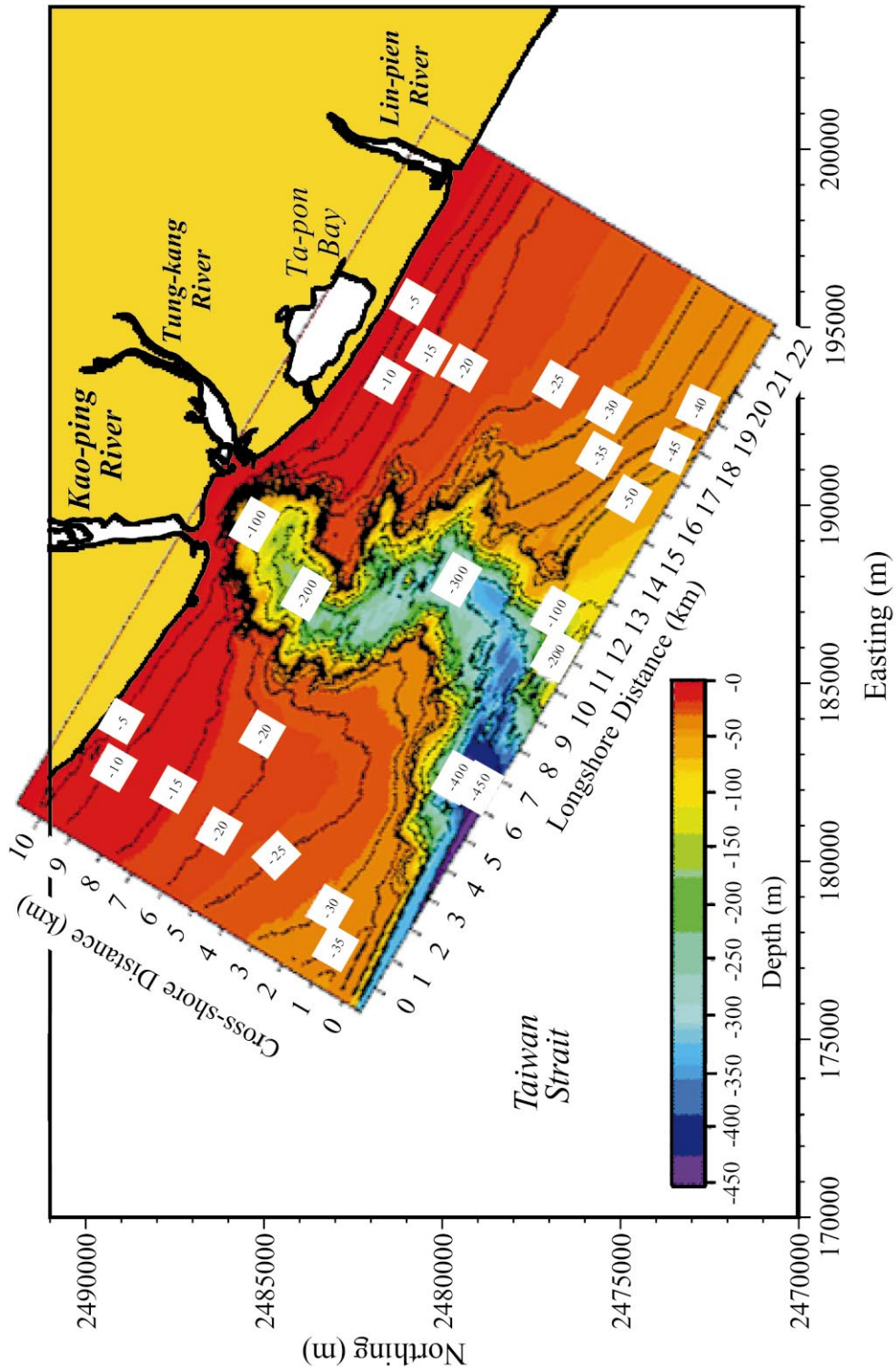


Fig. 5. The surveyed bathymetry of the study area. The contours are in meters based on Kee-lung mean sea level. The color bar indicates the depth range.

also analyzed for the grain-size frequency distribution by using a Coulter LS 100 particle analyzer, and recorded at 31 μm (coarse-grained silt), 4 μm (mid- to fine-grained silt), and finer than 4 μm (clay). Consequently, the data set consisted of 23 grain sizes (20 sand classes plus three mud classes). The abundance of each grain size in the study area was then plotted over the bathymetric contours following the same coordinate transformation procedure so that the morpho-textural characteristics can be fully visualized.

3.1.3. Hydrographic survey and suspended sediment concentration (SSC) analysis

Six hydrographic surveys along the axis of the submarine canyon were conducted in 1999 and 2000. During the flood season of 1999, the surveys were spaced roughly 1 month apart in June, July, and August. During the ensuing dry season, the surveys were spaced about 10 weeks apart in October, 1999, January and March, 2000 (Fig. 3a). A comparison between the monthly discharge for 1999 and 2000 (up to March) and the 41-yr (1949–1990) mean monthly discharge shows that the river runoff in the flood season of 1999 was higher than the mean, especially for August (Fig. 3b), suggesting greater-than-average influence of the river on the coastal sea. There were 10 hydrographic stations on each survey (Fig. 4). The spacing between the stations was about 2 km, except in the middle section of the surveyed region where the spacing was 1 km. At each station, profiles of conductivity, temperature, and light transmission were measured using a Sea Bird SBE 9/11 CTD system. Three water samples at the surface, mid-depth, and 20 m from the seafloor were also taken.

Each seawater sample was filtered through a pre-weighed membrane filter (Nucleopore PC, 1.2 μm), driven by a peristaltic pump. After filtration, the residue on the filter was washed with deionized distilled water to remove sea salt. The washed filter was dried in an oven at 60°C and then re-weighed with an electronic balance (Mettler AT20) to determine the concentration. Linear regression analysis was performed between the SSC values and the corresponding light transmis-

sion measurements to subsequently convert light transmission values to SSC values in mg/l.

3.2. Field work results

3.2.1. Bathymetry

The bathymetric contours of the study area indicate a meandering head region of the Kao-ping Submarine Canyon incising into an otherwise gentle-sloping shoreface and inner shelf (Fig. 5). The landward terminus of the canyon starts at about 1 km seaward from the mouths of both rivers where the water depth increases abruptly to exceed 100 m. The canyon is surrounded by steep walls with jagged outlines. The floor of the canyon deepens seaward, and thus the drop between the edge of the canyon and the canyon floor increases seaward.

3.2.2. Grain-size distribution patterns

Only the plots of distribution patterns of six representative grain sizes are presented to reveal the full range of morpho-textural variations of grain-size data (Fig. 6). Very coarse-grained sands (represented by 1.41 mm) are relatively scarce in the study area. They only appear in a small area on the right-hand side (facing seaward) of the Kao-ping River mouth near the head of the canyon. Coarse-grained sands (represented by 0.59 mm) are a little more abundant than the previous fraction. They appear additionally on the shoreface on the right-hand side of the river mouth, and in the deeper (around 450 m) part of the canyon. Medium-grained sands (represented by 0.30 mm) are mostly abundant on the shoreface outside of the canyon. They also tend to be wider distributed on the right-hand side of the river mouth. Fine-grained sands (represented by 0.15 mm) are the most abundant group in the sand fraction. They are virtually devoid inside the canyon. Very fine-grained sands (represented by 0.074 mm) are the most uniformly distributed group in the sand fraction in the whole study area. The abundance of mud shows that (1) they have elevated concentrations (at certain locations, exceeding 90% by weight) inside the canyon, (2) they are more abundant in greater depths in the canyon, and (3) their abundance

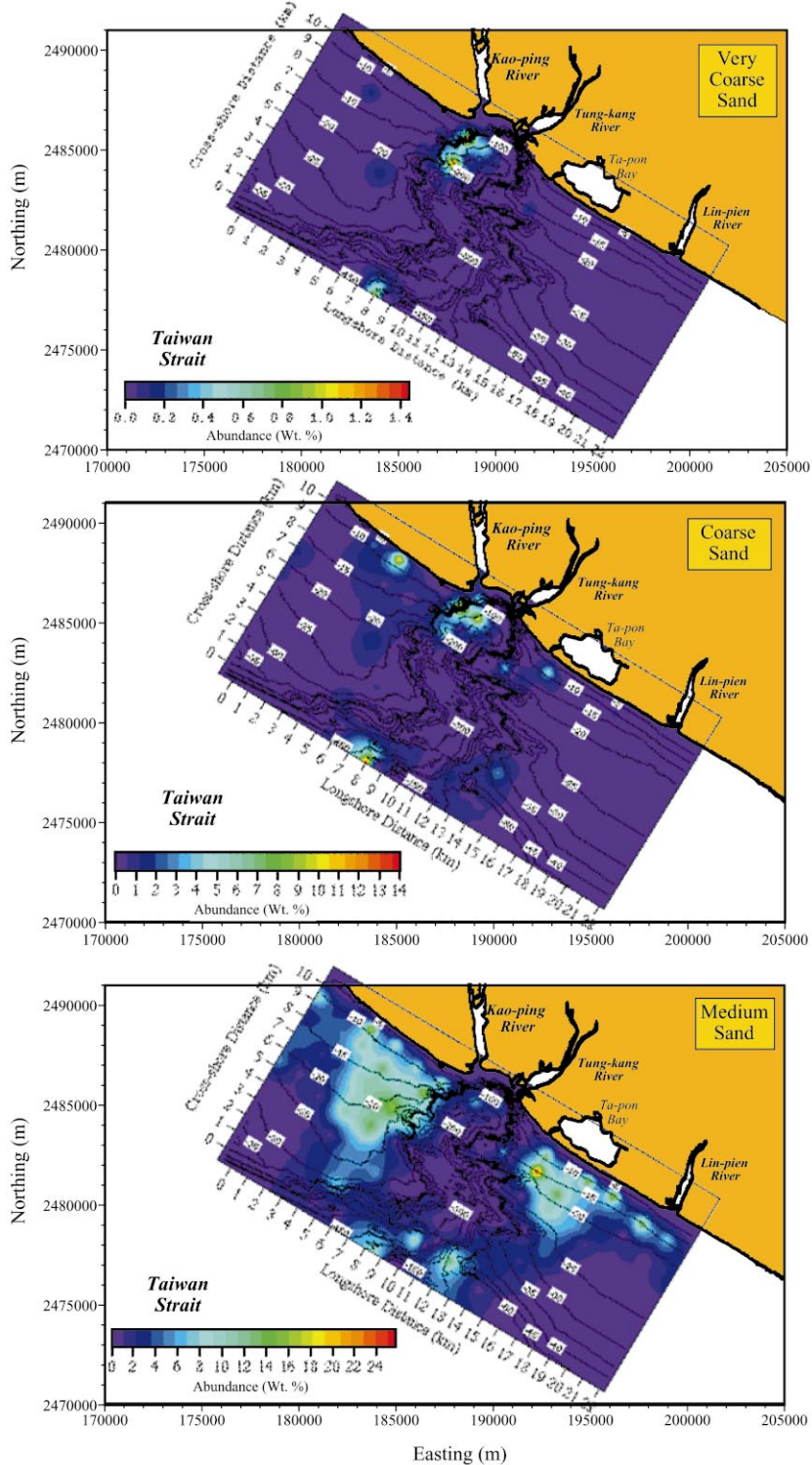


Fig. 6. Plots of distribution patterns over the bathymetric contours of six grain-size classes representing very coarse sand (1.41 mm), coarse sand (0.59 mm), medium sand (0.30 mm), fine sand (0.15 mm), very fine sand (0.074 mm), and mud (finer than 0.063 mm), respectively. The range of abundance of each size class in percent weight is indicated by the color bar in each plot.

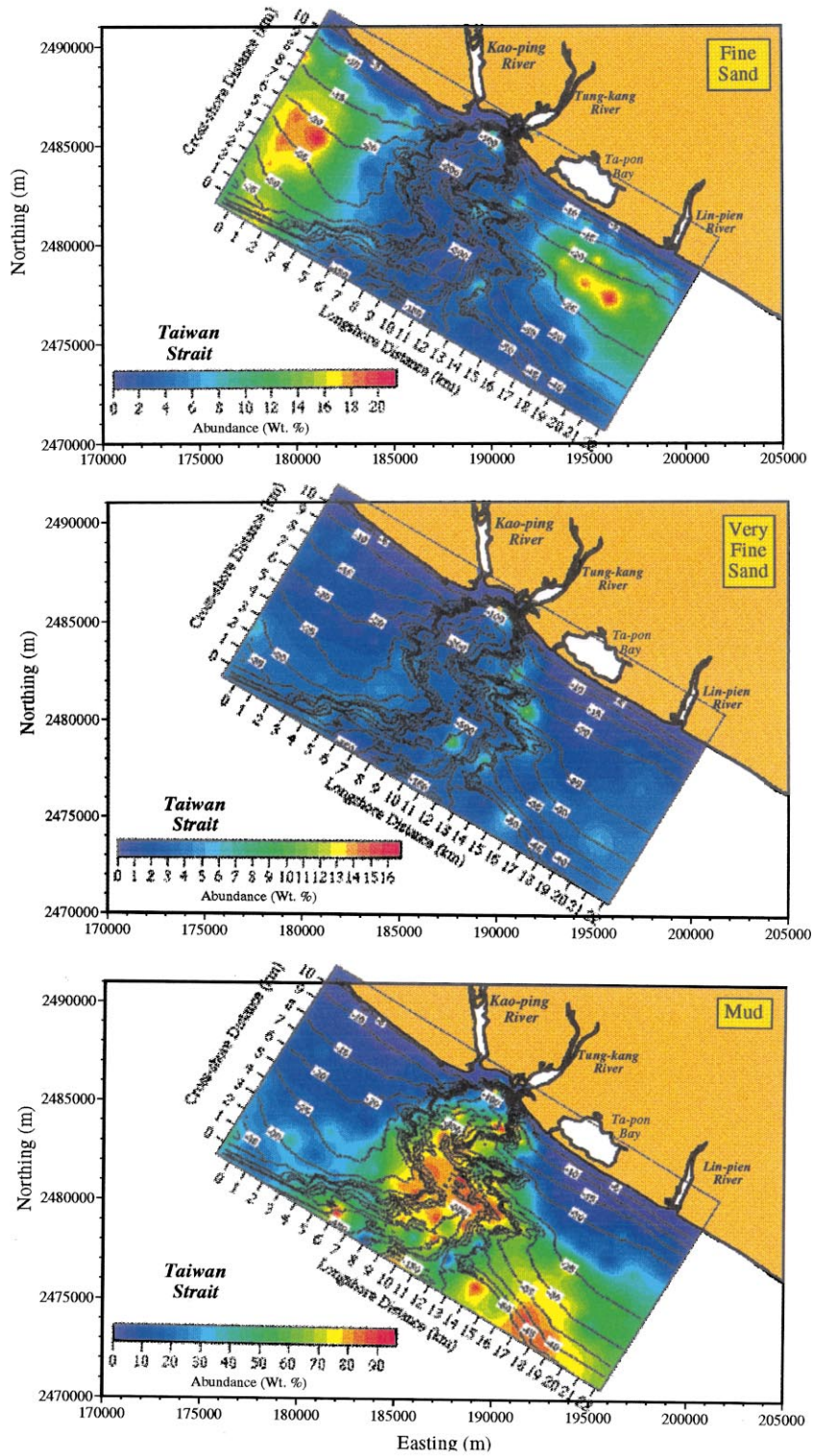


Fig. 6 (Continued).

displays a NW–SE trend following that of the canyon axis.

Due to the overwhelming appearance of mud inside the canyon, the abundance of mud was further broken down into the distributions of the coarse-grained silt (63 to 31 μm), the medium- to fine-grained silt (31 to 4 μm), and clay (finer than 4 μm). The results showed that the mud group is dominated by medium- to fine-grained silt.

3.2.3. Seasonal hydrographic characteristics in the Kao-ping Submarine Canyon

A distinct seasonal pattern can be established within the surveyed area of the Kao-ping Submarine Canyon based on the T – S diagram for each hydrographic survey (Fig. 7). The surveyed salinity and temperature characteristics are basically caused by the presence of the warm, brackish river effluent (Fig. 7b,c) and the cold, salty canyon water (Fig. 7e,f). The T – S characteristics show a strong river signal in the August 1999 survey (Fig. 7c), which coincided with above-average monthly discharge of the Kao-ping River (Fig. 3).

The distribution of SSC (whose abundance is indicated by the color bar) and the seawater density structure (as sigma- t contours) for each survey are plotted in a 2-D frame representing a vertical plane that zigzags along the axis of the submarine canyon (Fig. 8). Since it usually took 4–5 h to complete the entire hydrographic transect, the sequential data collected along the transect are influenced by different phases of the tide in the canyon. Therefore, these plots should be considered as tidally aliased quasi-snapshots of the canyon at six different times of the year.

Despite of the seasonal difference, the Kao-ping Submarine Canyon is a stratified environment as indicated by isopycnals (Fig. 8). On several occasions, density perturbations were observed as indicated by loops of isopycnals (Fig. 8a,b,d). These perturbations are associated with perturbations in the temperature field caused by pools of cold water (not shown).

Although the hydrographic surveys were conducted during flood and dry seasons and at different tidal stages, all the observed SSC distributions

share the following common characteristics. (1) There are localized spots of high SSC in the bottom nepheloid layer (Fig. 8). These locations generally fall within the shallower area of the canyon indicated by the box in Fig. 4. (2) Higher SSC values are generally in the lower part of the water column. Except for the two flood season surveys (Fig. 8a,b), higher SSC values also tend to occur toward the seaward end of the canyon. During the flood season, suspended sediments carried by the river effluent are evident in the upper part of the water column near the head of the canyon (Fig. 8a–c). It is worth noting that the density field and the SSC distributions seem to be correlated as indicated by the coincidence of concentrated SSC spots with density perturbations (Fig. 8a,b). In addition, on one occasion in July, 1999 (Fig. 8b), the distribution of suspended sediment seems to follow the isopycnal surfaces.

In general, the six hydrographic surveys have reasonably established the intra-seasonal hydrographic characteristics in the Kao-ping Submarine Canyon. The canyon is filled with cold and salty offshore water that is little affected by the change of seasons. During the flood season of the Kao-ping River, the river effluent expands seaward over the canyon. However, no effective mixing takes place between the two water masses. Because of the plume water, the density stratification in the canyon region is intensified during the river flood season.

3.2.4. Static stability in the Kao-ping Submarine Canyon

Since the SSC field in the submarine canyon is to some extent related to the density field, it is important to quantify the density structure in the canyon by computing the static stability (E) according to (Knauss, 1978):

$$E = -1/\rho_o(d\rho/dz) \quad (1)$$

where ρ_o is the reference density of seawater, and $d\rho/dz$ is the vertical density gradient. The computed E value was then contoured and plotted over the SSC distribution for comparison (Fig. 9). Positive E values indicate static stability,

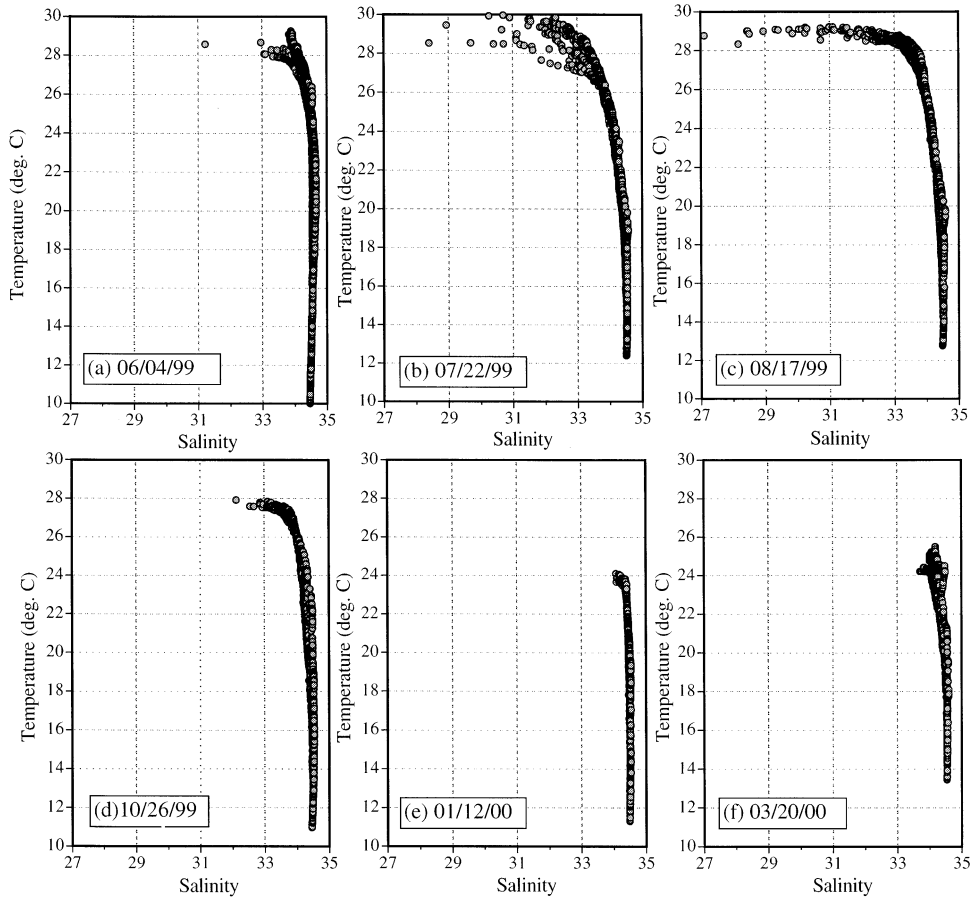


Fig. 7. *T-S* diagram based on survey data on (a) June 4, (b) July 22, (c) August 17, (d) October 26, 1999, (e) January 12, and (f) March 20, 2000.

negative *E* values indicate static instability in the water column. Results show that the water column in the canyon has greater stability in the summer (Fig. 9b,c). The whole water column is less stable in the winter and spring (Fig. 9e,f). During the transition in the fall, the stability in the upper water column remains high, yet the lower water column becomes less stable (Fig. 9d). It is noticeable that near-bottom localized high SSC spots are associated with regions of instability in the summer (Fig. 9a–c) and fall (Fig. 9d) transects. As the overall stability of the water column relaxes in the winter, the near-bottom localized high SSC spots are no longer related to the water column instability. This suggests a seasonal factor that controls the coupling between these localized

high SSC features and the density structure in the canyon.

3.2.5. Inferred generation and propagation of internal tide in the canyon

Since the local topography (slope) of the shelf affects the energy flux of the internal tide (Sherwin and Taylor, 1990), different potential modes of internal tide propagation in the Kao-ping Submarine Canyon are investigated by the ratio between the slope of the canyon floor (α) and the internal wave characteristics (Ribbe and Holloway, 2001):

$$s = \pm \left(\frac{\omega^2 - f^2}{N^2 - \omega^2} \right)^{1/2} \quad (2)$$

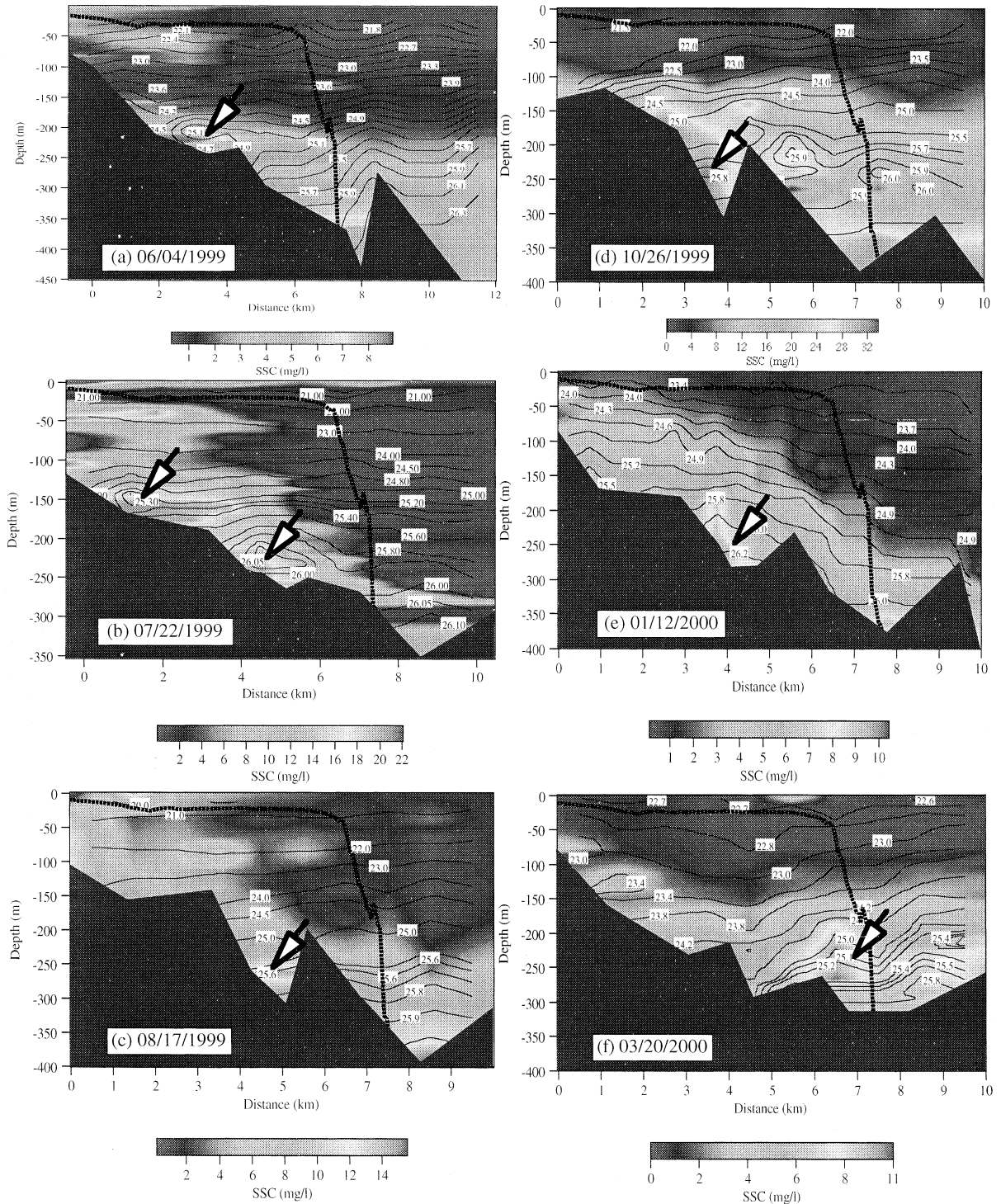


Fig. 8. Contoured isopycnals (σ_t) plotted over the SSC (in mg/l), whose range is indicated by the color bar below, surveyed on (a) June 4, (b) July 22, (c) August 17, (d) October 26, 1999, (e) January 12, and (f) March 20, 2000, along the Kao-ping Submarine Canyon axis. The thick dashed curve delineates the upper and seaward boundary of the surveyed portion of the submarine canyon. The horizontal distance in each plot is relative to the most landward hydrographic station on each transect (zero distance). The depth values used in the seafloor masking were the actually echo sounding depths recorded at the end of each profiling operation by the drifting vessel. Arrows point to locations where high SSC spots in lower water column occurred.

where ω is the frequency of the M_2 tide, f ($5.56 \times 10^{-5} \text{ s}^{-1}$) is the Coriolis parameter, and N is the buoyancy frequency ($N^2 = gE$, g being the gravitational acceleration). If $\alpha/s > 1$ (supercritical bottom slope), much of the internal tide energy is reflected back toward the sea, if $\alpha/s < 1$ (subcritical bottom slope), the canyon floor allows the energy to propagate toward the head of canyon, and if $\alpha/s = 1$ (critical bottom slope), the generation of internal wave is the strongest (Baines, 1982; Ribbe and Holloway, 2001). Since there are 10 hydrographic stations on each transect, the slope calculation of the canyon floor was divided into nine segments. The sign for each segment is positive for seaward-dipping slope and negative for landward-dipping slope. The value of N in Eq. 2 was computed based on the interpreted values of E (Eq. 1) shown in Fig. 9.

The results of α/s reveal seasonal variability of the influence of seafloor topography on the internal tide generation and propagation in the Kao-ping Submarine Canyon (Fig. 10). Critical and supercritical conditions (positive values) only exist in the middle section of the transect for the July, and August, 1999 transects (Fig. 10b,c). This suggests that (1) the presence of internal tide is more likely in the flood season, and (2) the headward propagating internal tide is more likely to be reflected seaward in the middle section of the surveyed canyon based on the slope of the canyon floor. The negative supercritical slopes also suggest the possibility of secondary reflection of seaward-reflected internal tide. Furthermore, if the effect of the canyon wall is taken into consideration, the two-way reflection of internal tide in this section would be even more likely due to the orientation change of the canyon axis. The implication of the internal tide on the sediment dynam-

ics in the canyon will be discussed later in this paper.

4. Methods for grain-size pattern analysis

4.1. Filtering concept and empirical orthogonal (*eigen*) function (EOF) analysis

Conceptually, factors influencing the grain-size distribution patterns in the study area fall into two major categories, i.e. where the sediments come from (sources) and how they are moved about (sediment transport and deposition processes). The observed morpho-textural relationship between grain-size patterns and the bathymetry is the result of the interplay of the above two categories through time (Liu and Hou, 1997; Liu et al., 2000). The challenge at hand is to decipher the meaningful information contained in the observed grain-size information. Subsequently, we propose several factors that might have exerted influence on the observed grain-size patterns in the study area. Within the study area, the Kao-ping Submarine Canyon is likely a conduit for both seaward and landward sediment transport. Sediments delivered to the study area at the northernmost and southernmost boundaries (via southeastward and northwestward alongshore sediment transports, respectively) are the effect of in-situ wave sorting and reworking. In order to minimize artificial variability, samples having common distinctive grain-size characteristics were carefully selected to represent each factor. We will briefly discuss each of these factors.

4.1.1. Sediments discharged by the Kao-ping River (a point source)

It is intuitive to assume that sediment dis-

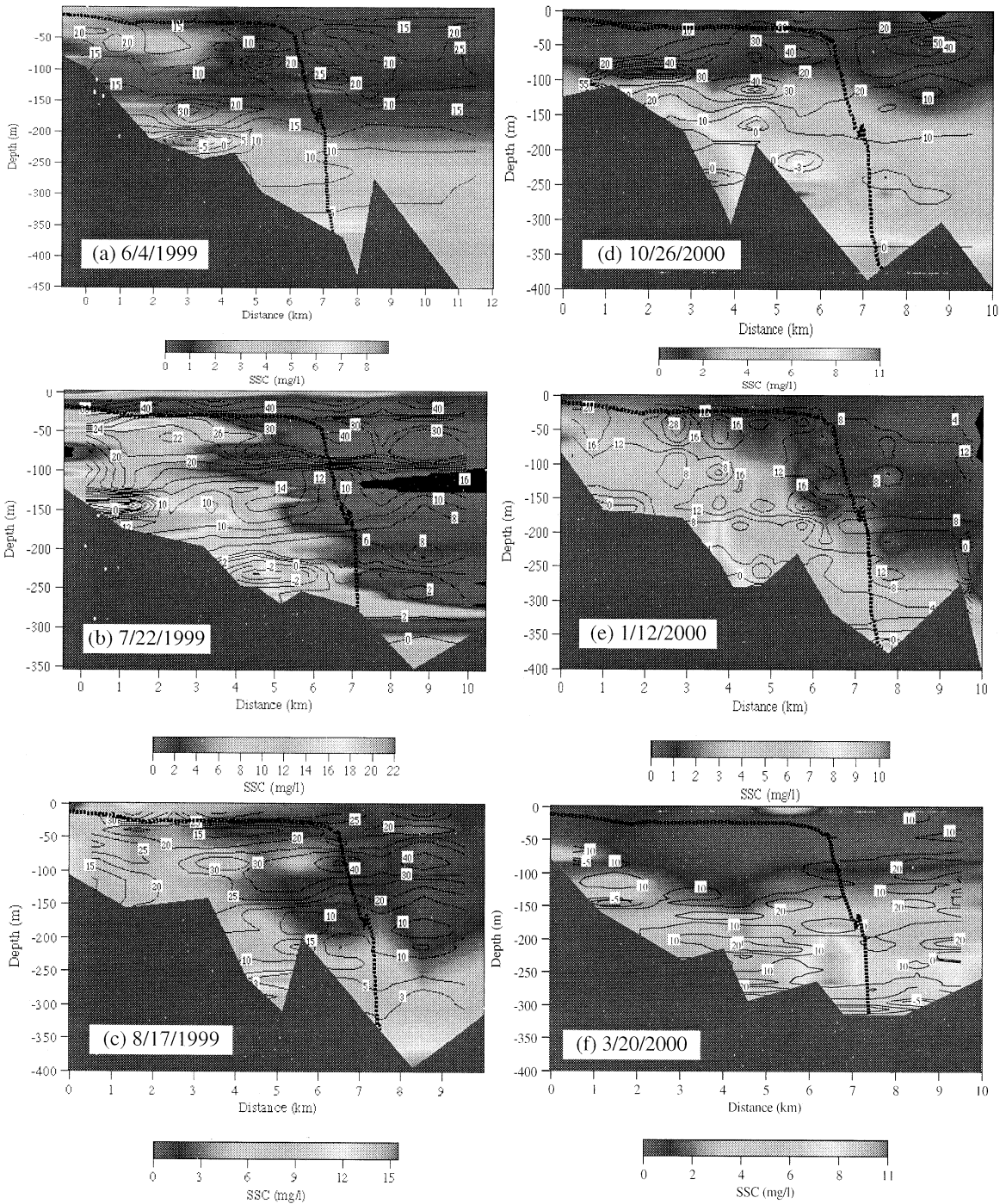


Fig. 9. Contoured static stability (E) plotted over the SSC (in mg/l), whose range is indicated by the color bar below, surveyed on (a) June 4, (b) July 22, (c) August 17, (d) October 26, 1999, (e) January 12, and (f) March 20, 2000, along the Kao-ping Submarine Canyon axis. Negative values indicate areas of static instability. The horizontal distance, the outline of the canyon, and the depth masking are the same as Fig. 8.

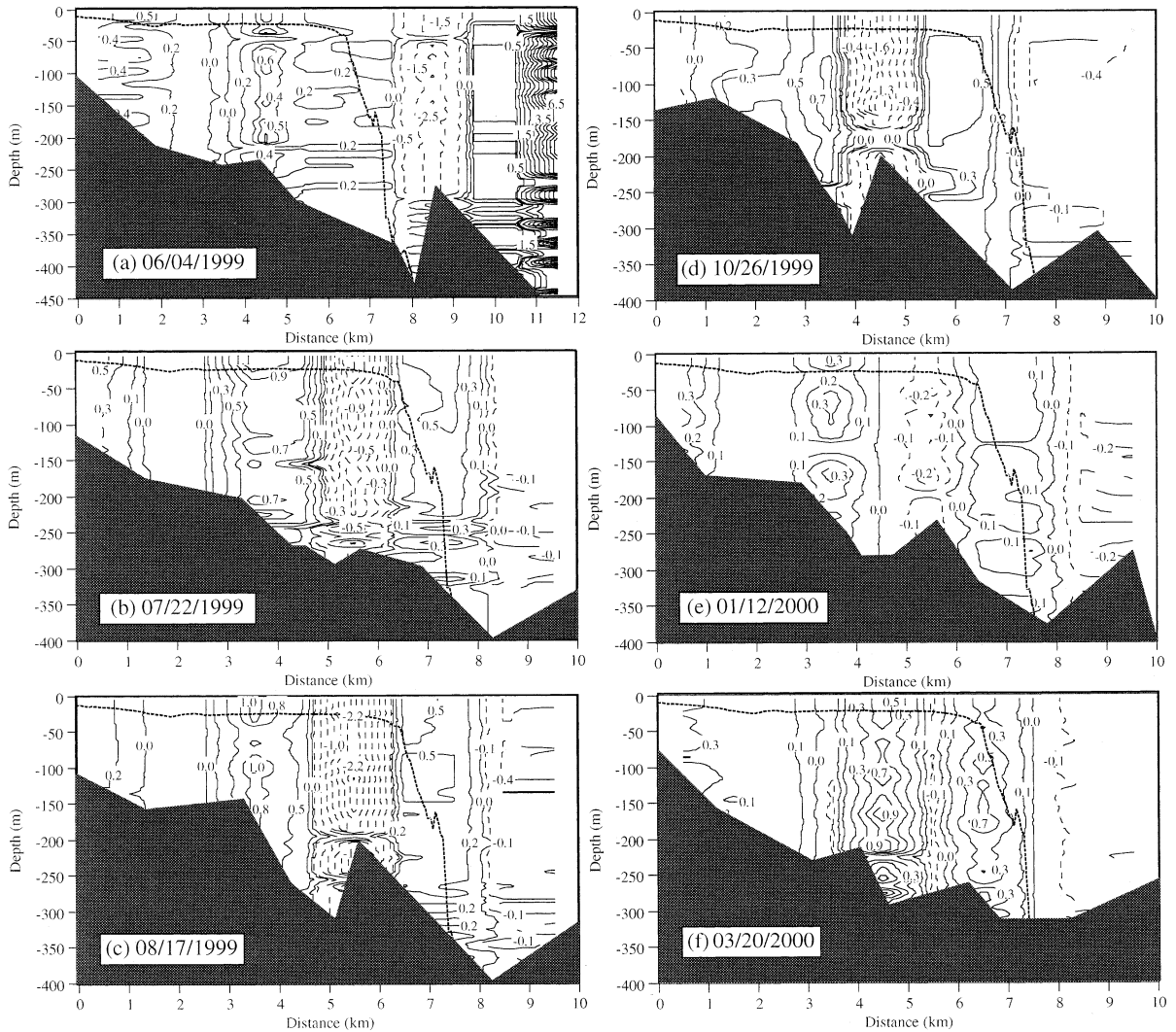


Fig. 10. Contoured α/s for transects surveyed on (a) June 4, (b) July 22, (c) August 17, (d) October 26, 1999, (e) January 12, and (f) March 20, 2000, along the Kao-ping Submarine Canyon axis. a = slope of canyon floor, s = internal wave characteristics. For explanation, see text. Dashed curves are negative values due to landward-dipping slope. The horizontal distance, the outline of the canyon, and the depth masking are the same as Fig. 8.

charged by the Kao-ping River would eventually settle on the seafloor within the sampled area. The grain-size composition of this hypothetical factor is represented by the average grain-size frequency composition of the sediment samples taken from the river bed inside the river mouth. It is apparent that the grain-size signal from the river is dominated by fine-grained sediments whose mud (silt

and clay) content exceeds 50% by weight (Fig. 11). The sand fraction of the river discharge is dominated by fine- to very fine-grained sands.

4.1.2. Sediment entering the submarine canyon from the seaward end (a point source)

This factor is represented by the average grain-size composition of samples located at the sea-

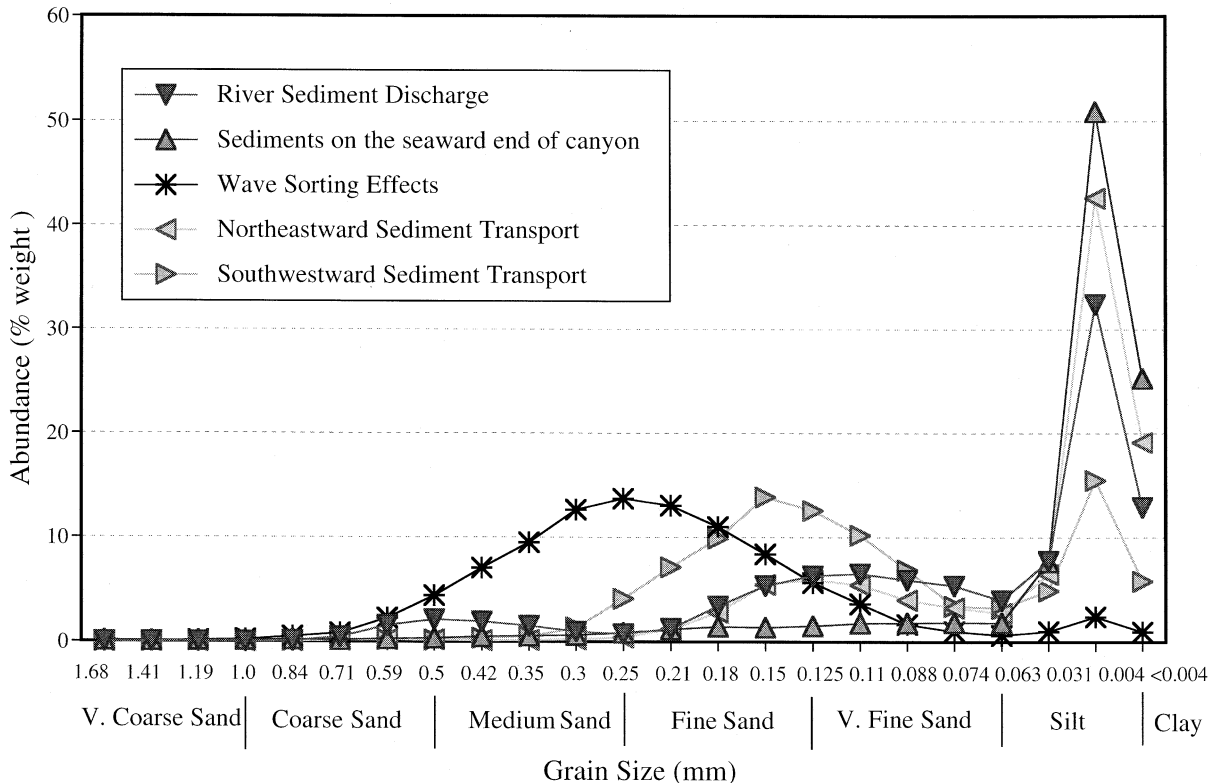


Fig. 11. Grain-size composition of the five hypothetical factors.

ward end of the submarine canyon in the study area. The textural makeup of this factor contains over 80% of mud (Fig. 11).

4.1.3. The effect of wave sorting (reworking)

The sorting by shoaling waves is the primary mechanism for sediment reworking on wave-dominated shoreface (Liu and Hou, 1997; Liu and Zarillo, 1990; Liu et al., 2000). Wave sorting can be visualized by the progressive changes in the individual grain-size abundance pattern from the beach seaward to the inner shelf (Liu and Zarillo, 1989; Liu et al., 2000). In this study, the effect of wave sorting can be visualized by the variations of the grain-size composition in all the 19 samples (last sample on each shore-parallel transect) (Fig. 2). The water depths at these sample locations represent a typical profile of the upward concave shoreface and gentle-sloping in-

ner shelf (Fig. 12a). There is the general trend of decreasing sand content and increasing mud content in the seaward direction (Fig. 12b). Also, within this general trend, the modal size in the sand fraction becomes progressively finer (Fig. 12b). Consequently, we took the average of the grain-size frequency distributions of all samples outside the canyon region that were shallower than 10 m to represent the effect of wave sorting. The resulting grain-size curve shows a Gaussian distribution in the sand fraction and a small mud 'tail' (Fig. 11), which is similar to what Liu et al. (2000) found.

4.1.4. Northwestward alongshore transport (a line source)

As suggested by the seasonality of the incident wave field and nearshore current field (Fig. 2), both northwestward and southeastward sediment

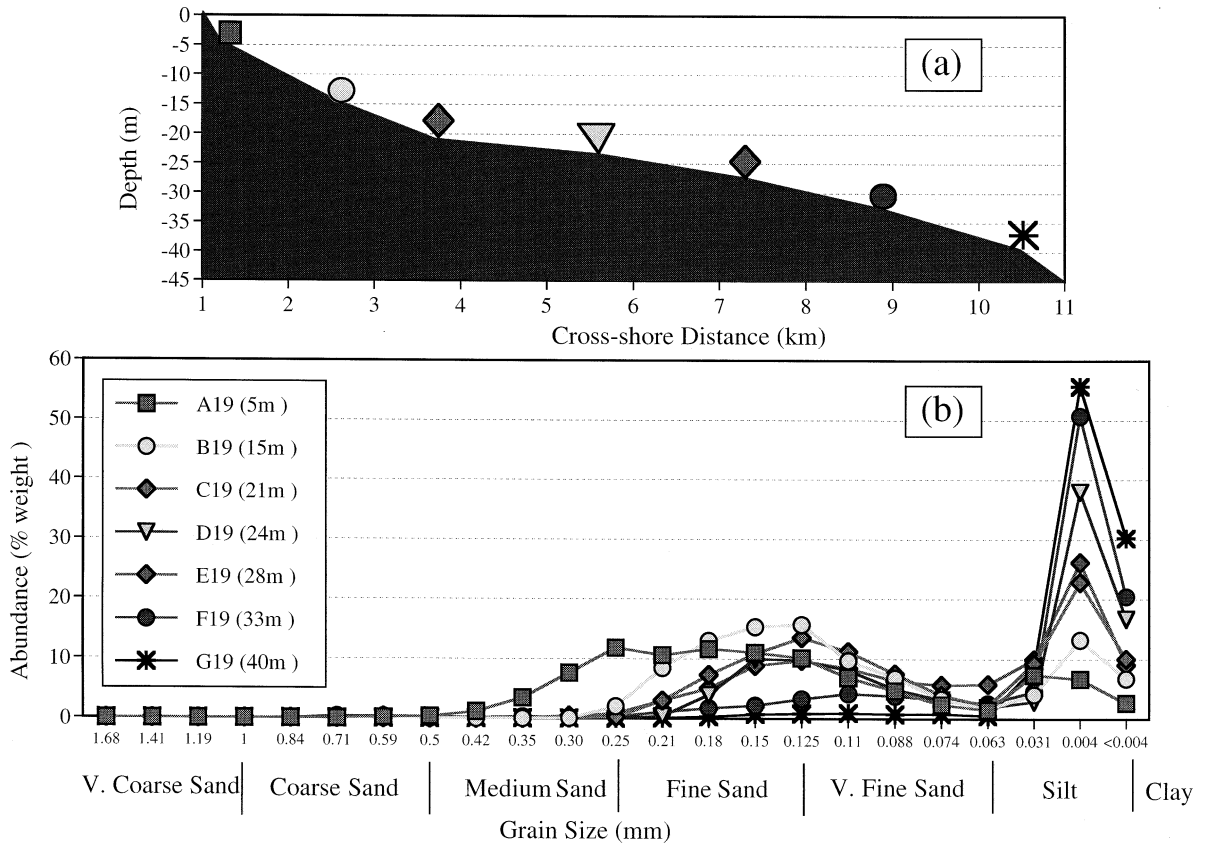


Fig. 12. (a) The plot of water depths of all 19 samples of all seven sediment transects across the shoreface and inner shelf. (b) Grain-size composition curves of all 19 samples. The numbers in the parentheses in the legend indicate the water depths at which the samples were taken.

transports are likely to take place. Therefore, sediment patterns in the study area could be influenced by the transport of sediments that entered the study area at the southernmost boundary. This possible source is largely composed of fine-grained materials (Fig. 11).

4.1.5. Southeastward alongshore transport (a line source)

By the same token, sediments that enter the study area at the northernmost boundary are also a likely source. This hypothetical source is characterized by an overall bi-modal distribution, very different from the hypothetical source from the south (Fig. 11).

To test the above hypotheses and minimize this complexity, an analytical methodology using the

combination of ‘filtering’ and the EOF analysis technique (Liu and Hou, 1997; Liu and Zarillo, 1990; Liu et al., 2000) was used (Fig. 13).

4.2. McLaren Model and transport vector method

McLaren (1981) pointed out that trends in the spatial variations of mean grain size, sorting, and skewness (in phi units) can be useful to identify both the probable source and the probable deposit, which in turn, can infer the net sediment transport paths. McLaren and Bowles (1985) take this concept further to develop a statistical model (referred to as the McLaren Model thereafter) that determines the transport direction by all possible pairs in a data set.

Another analysis technique of grain-size trends

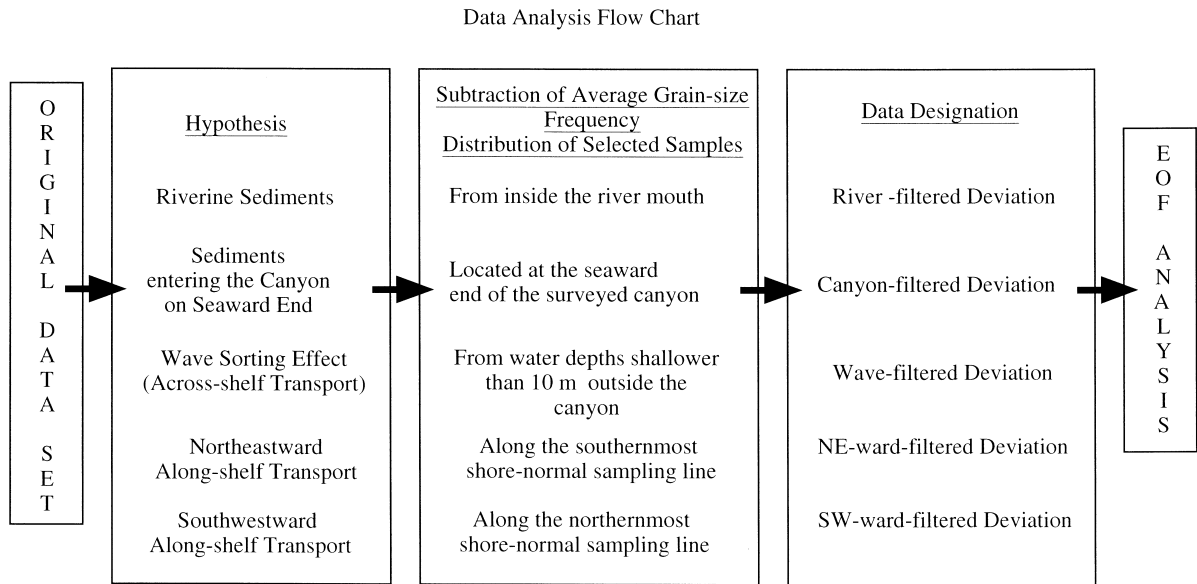


Fig. 13. The flow chart for the grain-size analysis using filtering and EOF technique.

using ‘transport vectors’ (Gao and Collins, 1992, 1994; Gao et al., 1994) was also used. This technique evaluates the existence of transport direction between a particular sample (site) with its neighboring samples (sites) the same way as the McLaren Model does. If either of the two transport cases exists between a pair of samples, a dimensionless ‘trend’ vector of unit length is defined (Gao and Collins, 1992, 1994; Gao et al., 1994). In the case where there was more than one unit length vector at one sample site, the vectorial sum of all the vectors is then produced. A transport vector is further produced by averaging over neighboring sites to represent residual pattern of transport direction (Gao and Collins, 1992). In

this study, a neighboring site is defined to be a sample site that is less than 1.2 km (the characteristic distance) away from the site of interest.

5. Results

5.1. EOF analysis

The deviations explained by the first two eigenmodes of all deviation fields are listed in Table 1. When judged by the first mode alone, the deviation fields of wave-sorting effect, sediments are the seaward end of the canyon, and the northwestward alongshore transport has no-

Table 1
Percentage of data explained by the first two eigenmodes

Deviation field	First mode	Second mode	Cumulative
Across-shelf transport (wave sorting)	88.2	6.3	94.5
Sediments on the seaward end of the canyon	87.7	5.4	93.1
Northwestward alongshore transport	81.9	8.3	90.2
Southeastward alongshore transport	74.9	15.1	90.0
River sediment discharge	72.6	11.8	84.4
Unfiltered data	74.1	10.9	85.0

ticeably improved correlation over the original unfiltered data set. The deviation field of the southeastward alongshore transport has a slight improvement, and that of the river sediment discharge actually becomes degraded (explains less amount of data than the unfiltered). When both modes are concerned, the wave-sorting effect and the sediments at the seaward end of the canyon are the two most important factors influencing the observed grain-size patterns. This implies that the agitation of the seafloor by shoaling waves is the most important mechanism affecting the movement and transport of grain sizes in the study area. Sediments (mostly mud) entering the submarine canyon at the seaward opening is the most important sediment source in the study area. The northwestward direction is the dominant direction of alongshore sediment transport in the study area. It was unexpected that the sediments discharged by the Kao-ping River turned out not to be the most important influencing factor in the study area.

The eigen characteristics of the three most important deviations are plotted in Fig. 14. The first three panels are the plot of eigenvectors for the wave sorting (Fig. 14a), sediment influence at the seaward end of the canyon (Fig. 14b), and northwestward alongshore transport (Fig. 14c), respectively. In all these three deviation fields, the eigenvectors divide the 23 grain-size classes into two groups according to the sign. The positive group includes the mud, and the negative group is dominated by the fine-grained sand fraction. The spatial correspondence of these two groups is visualized by the contour plot of eigenweightings (Fig. 14d–f). The positively weighted group is contoured by solid lines, and the negatively weighted group is contoured by dashed lines.

The spatial eigen characteristics of the wave-sorting deviation field (Fig. 14d) suggest that the deviations are primarily caused by the presence of mud (positive group) in the study area. On the other hand, the fine-grained sand group is the primary cause in the landward canyon transport deviations field (Fig. 14e). The absence of contour lines inside the canyon and in the shoreface region north of the canyon suggests homogeneity. There

is a clear spatial demarcation of the two groups in the northwestward alongshore transport deviation field (Fig. 14f). The mud group is closely associated with the submarine canyon, whereas the fine sand group is associated with the shelf regions outside the canyon.

5.2. Transport directions based on the McLaren Model

In a schematic diagram of the study area (Fig. 15), the existence of transport directions for the submarine canyon region and the regions of the shelf on the northwest and southeast sides of the canyon are represented by arrows. Each line of arrows were based on nine pairs of samples, respectively. Along the axis of the canyon, both low energy and high energy landward transport exist (Fig. 15). Only low energy transport exists in the seaward direction. On the shelf outside the canyon, only transports in shore-parallel directions were examined by the transect. On the northwest side of the canyon, both high and low energy transport in the northwestward direction exist on the lower shoreface and upper inner shelf. For the two occurrences that southeastward direction does exist, they are only in low energy transport. In general, the northwestward transport direction dominates. On the south side of the canyon, transport only exists on the deepest part of the study area, and the probability of northwestward transport is slightly greater than the southeastward transport.

5.3. Transport vector

The transport vector at each sampling site is plotted over the bathymetric contours in the study area (Fig. 16). In the landward region of the surveyed submarine canyon, transport vectors are predominantly pointing seaward. On the other hand, in the seaward region, the vectors are mostly pointing landward. There is a zone of convergence that separates these opposing arrows that corresponds to the dashed box in Fig. 4. Northward pointing arrows appear at all depths in the section northwest of the canyon. The vectors in the section southeast of the canyon are less

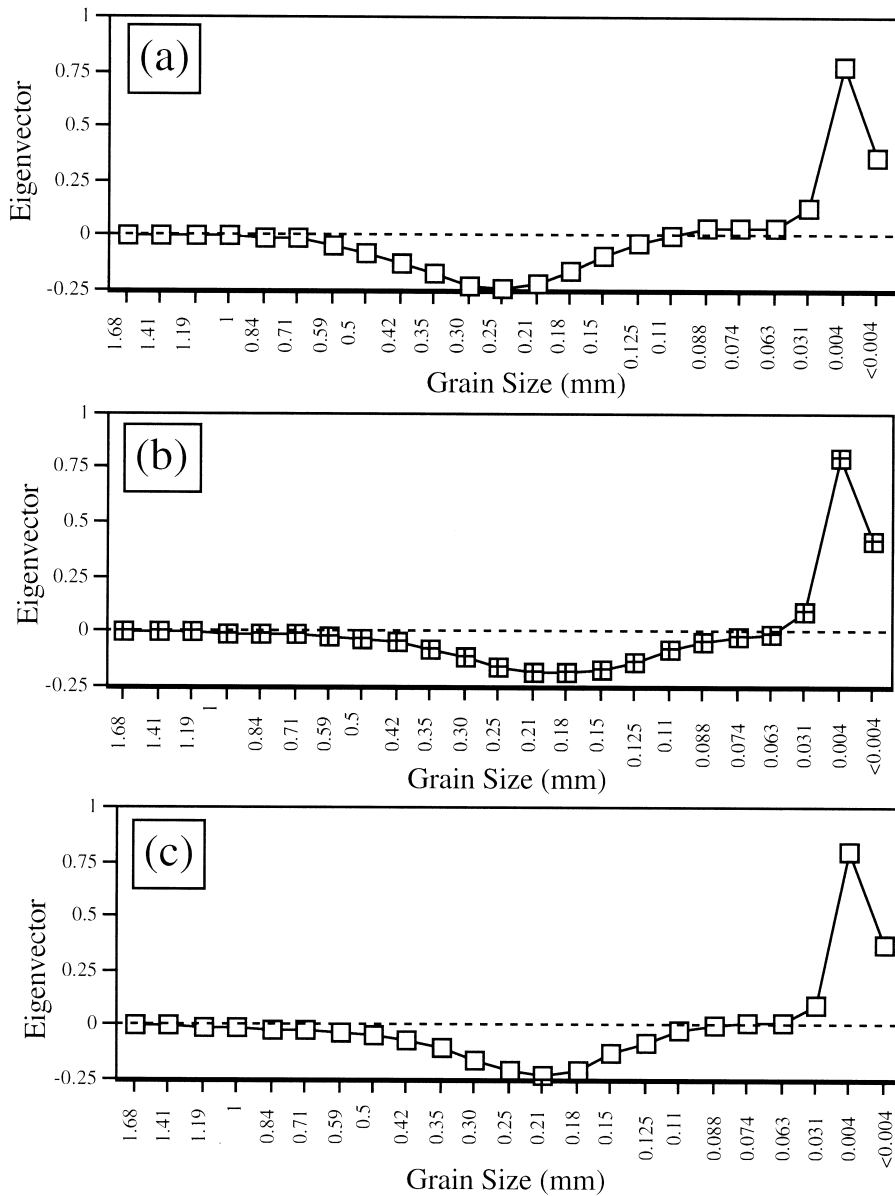
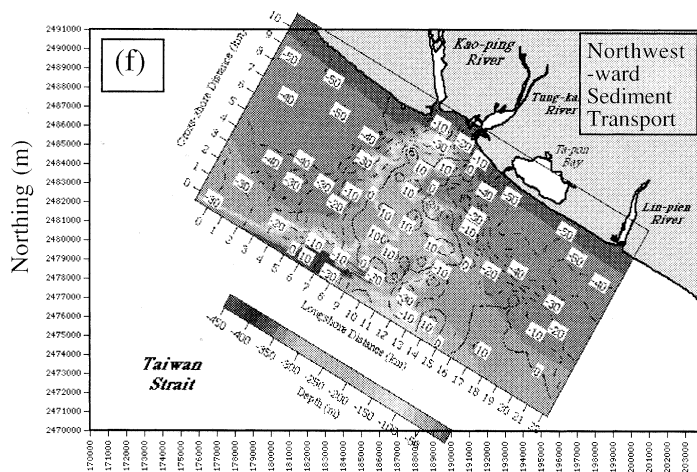
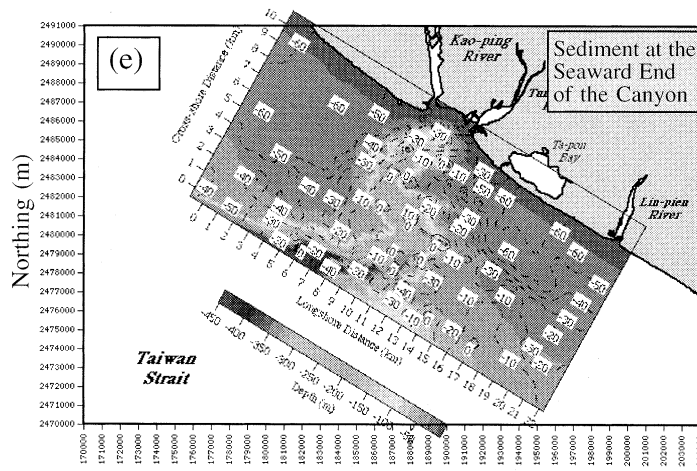
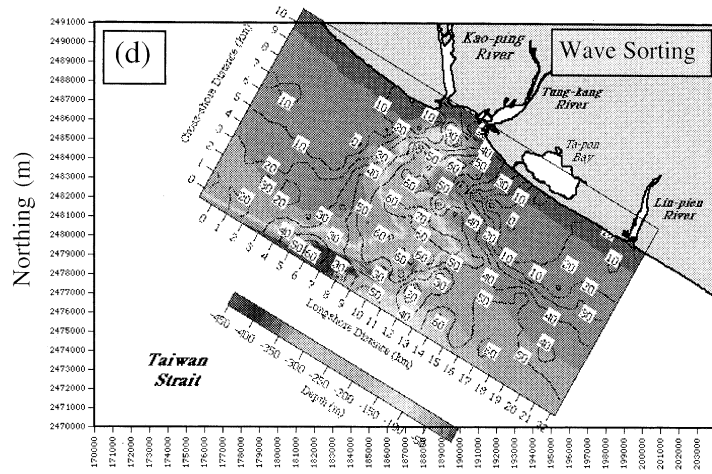


Fig. 14. The plots of eigenvectors for the (a) wave-filtered, (b) canyon-filtered, and (c) northwestward-filtered deviations, and the contour plots of the corresponding eigenweightings over the bathymetry (shaded) for the (d) wave-filtered, (e) canyon-filtered, and (f) northwestward-filtered deviations. The negative eigenweightings are contoured with dashed lines.

coherent in the longshore direction than its counterpart. There is a slight indication of seaward transport in the upper shoreface and strong likelihood of seaward transport in waters deeper than 40 m.

6. Discussion

It should be emphasized at the outset that both the EOF technique and the McLaren Model, of which the transport vector method is a derivative,



Northing (m)

Fig. 14. (Continued).

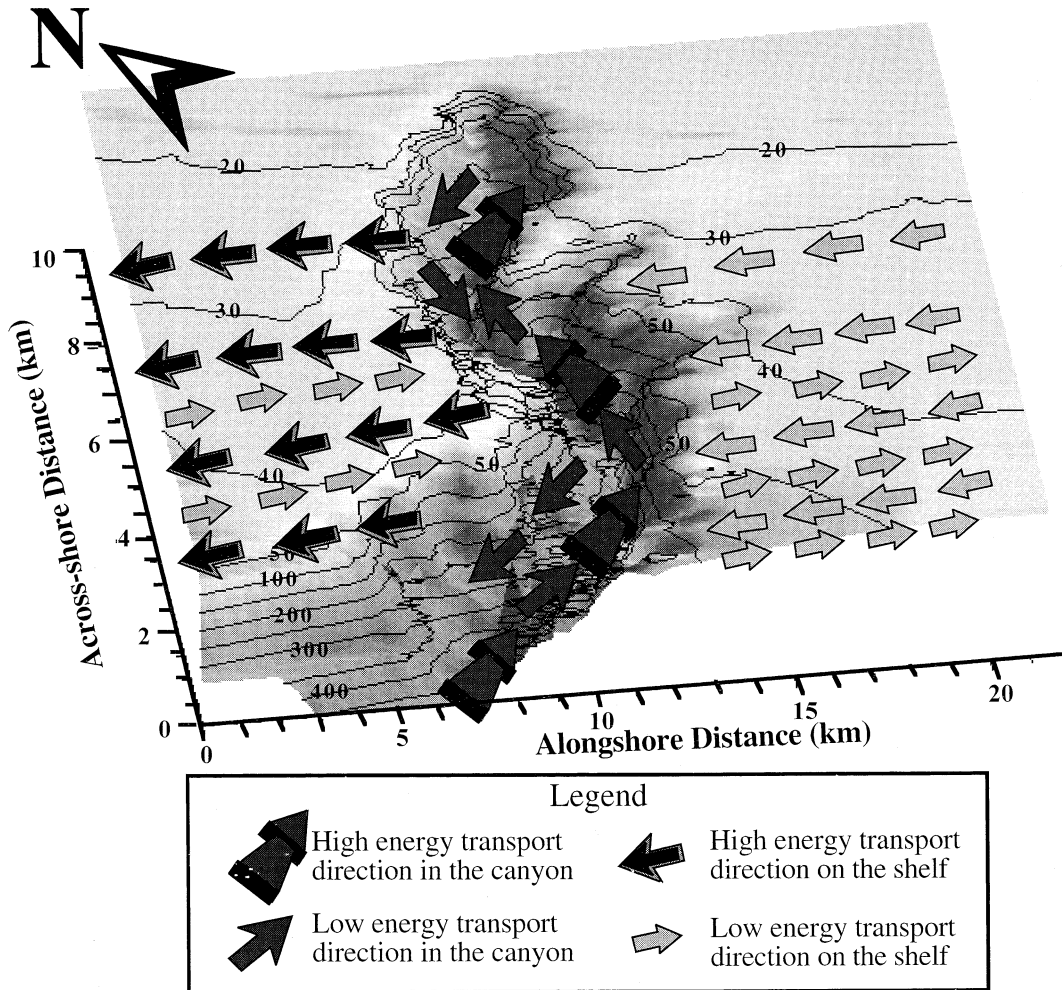


Fig. 15. Arrows in this diagram represent the existence of transport directions according to the McLaren Model analysis plotted over the 3-D bathymetry of the study area. Each line of arrows represents a predetermined orientation of transport. The isobaths are in meters.

are statistical methods. Both methods require a priori knowledge of the system and make intelligent yet subjective assumptions such as the influencing factors and possible sediment transport directions. The success of using the two methods depends not only on making the 'right' assumptions, but also on the inhomogeneity of the data set. If there was little spatial variability (trend) in the data, in other words, there was no contrast in the data set, either method would work. Furthermore, the EOF approach is empirical or data-

driven. The McLaren Model, however, is based on a number of assumptions (McLaren and Bowles, 1985).

The results of these two approaches in our study not only agree with one another, but also complement one another. The filtering and EOF method is able to rank the importance of different factors that influence the overall textural characteristics of the study area, which cannot be achieved by the McLaren Model. It also can distinguish the 'behavior' of different grain-size

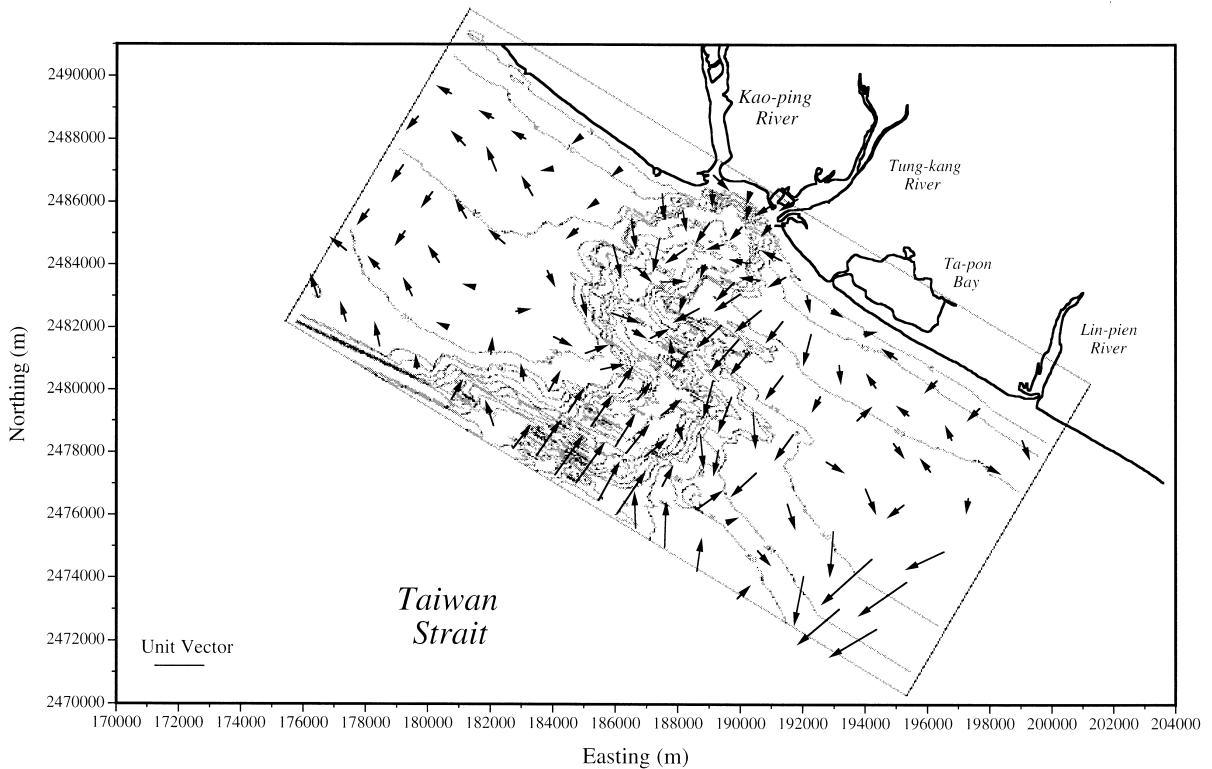


Fig. 16. Plot of transport vectors for each sampling site. The bathymetry is presented by unmarked contours.

groups and how the influencing factor in question affects their spatial characteristics. Yet, this method is unable to provide detailed inferred sediment transport pathways.

Although the McLaren Model is able to determine the existence of transport direction in the pre-determined orientation, the results are still vague. The transport vector method is, however, able to produce a map that makes the abstract findings intuitive. The plot of arrows also enables one to visualize the different transport pathways, which in turn, makes it easier to interpret with known or referred sediment transport processes.

All the three methods affirm that the Kao-ping Submarine Canyon is a sediment conduit that traps mud. The EOF method suggests that the sediment entering the canyon at the seaward end is more important than that discharged by the river. It also points out that the mud group is highly weighted in the submarine canyon, imply-

ing that the submarine is a trap for mud. The McLaren Model suggests that the landward transport is more likely than the seaward transport in the canyon. This supports the EOF finding that the sediment at the seaward end of the canyon is an important source. The transport vectors indicate seaward sediment transport from the landward end and landward transport from the seaward end of the canyon, converging in the region where the observed mud abundance on the seafloor is the greatest and also high SSC spots often are observed near the sea bed. Furthermore, the spatial coincidence between the observed high SSC spots in the water column and maximum abundance of mud on the surface of the seafloor suggests some kind of coupling between the water column and the sea bed. The convergence and the SSC–mud coupling suggests a depocenter of mud inside the canyon.

A simple hypothesis is proposed to explain the

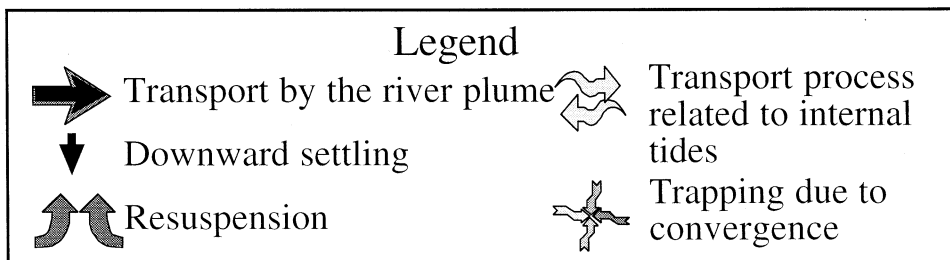
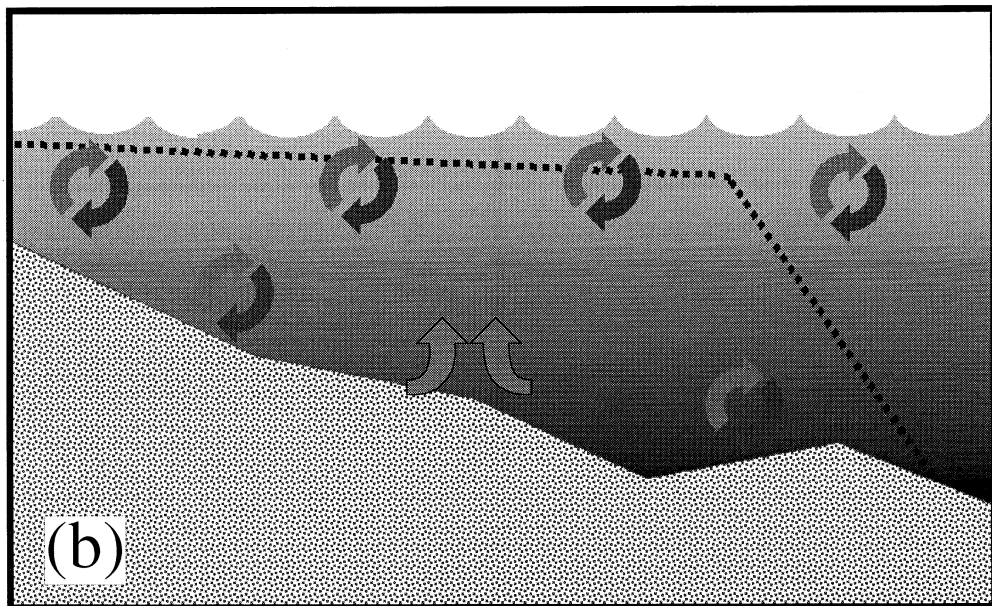
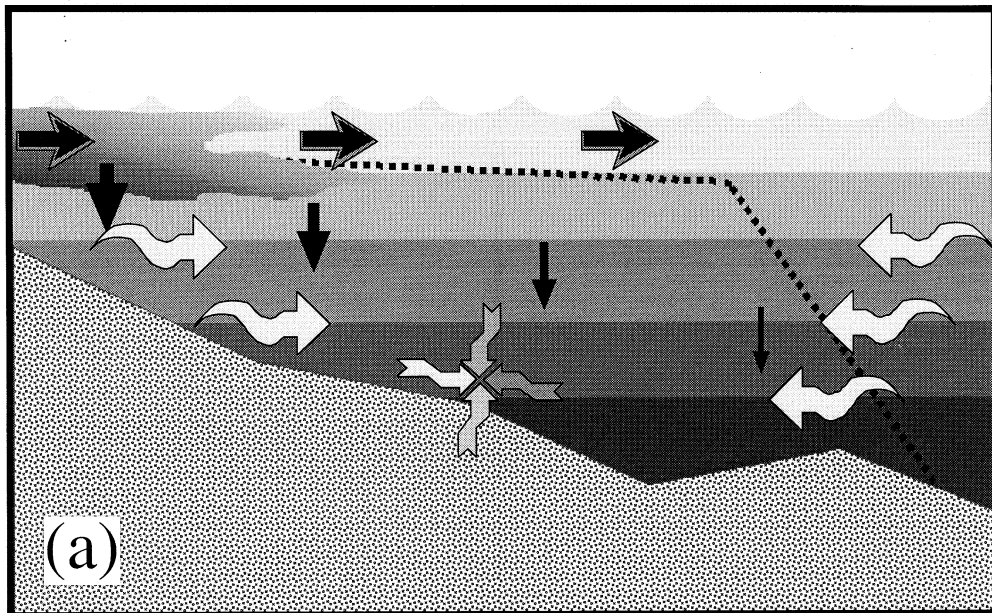


Fig. 17. Schematic diagram depicting the hypothesis regarding the hydrographic characteristics and the formation of high SSC spots inside the stratified Kao-ping Submarine Canyon for (a) flood season, and (b) dry season of the Kao-ping River.

seasonal variability of the hydrography and associated SSC in the Kao-ping Submarine Canyon (Fig. 17). The effects of barotropic tidal and subtidal flows, which might be important, are not considered at this point. The all-year-round stratification inside the canyon creates an overall statically stable environment that generally inhibits the agitation of sediments even as fine as mud, which is conducive to their trapping. During the flood season (summer), the sediment-laden river effluent delivers sediments (largely mud) to the coast and the head of the submarine canyon. Since the mean annual SSC of the Kao-ping River is 4.2 kg/m^3 (believed to be an overestimation), which is much smaller than the required value for forming hyperpycnal plumes ($35\text{--}45 \text{ kg/m}^3$, Skene et al., 1997), the effluent exits the river mouth most likely as the buoyant plume (Fig. 17a), similar to what we observed on June 4 and July 22, 1999 (Fig. 8a,b). The turbid yet buoyant plume water moves seaward sometimes following the isopycnal surfaces inside the canyon. As the river effluent diffuses, sediments settle gradually to the deeper part of the canyon and remain trapped.

Due to the well-developed stratification in the flood season, internal tides excited at the seaward end of the canyon or at the shelf break propagate landward through the canyon along isopycnal surfaces. Internal tides have been shown not only to create and maintain a nepheloid layer, they are also able to transport suspended sediments (Friedrichs and Wright, 1995). Under critical slope conditions, resuspension, deposition, and on-shelf sediment transport associated internal tides are the largest (Ribbe and Holloway, 2001). Therefore in the Kao-ping Submarine Canyon, internal tides could transport colder water and suspended sediments headward from the deeper part of the canyon. It is likely that some internal tide energy is trapped within the middle section of the canyon due to its geometry and bottom slope (Fig. 10). This high energy pocket

not only could cause perturbation (instability) in the density field, but also cause the SSC to concentrate forming the observed spots of high values. Consequently, internal tides and their trapping could provide an explanation for the observed concentration of mud on the seafloor, and the possibility of the depo-center (convergence) as suggested by the transport vector method. Furthermore, the on-shelf sediment transport by internal tides could also explain the dominant landward sediment transport inside the canyon suggested by the EOF method and McLaren Model.

During winter time (dry season thus little sediment input from the river), due to the deepening of the surface mixed layer, the water column in the canyon is less stratified. Consequently, internal tide-related transport is less pronounced. On the other hand, the relaxation of stratification is probably less inhibitive to the vertical transfer of momentum, which leads to localized resuspension of bottom sediment (Fig. 17b). This is probably a period of quiescence for sediment movement and transport.

A brief comparison is made with a similar study on the Tseng-wen River in southern Taiwan that also uses the EOF method (Liu et al., 2000). There are many physical similarities between the settings of the two study sites, including the magnitude and grain-size makeup (mud domination) of the river sediment discharge, the annual hydrological pattern of the river, the coastal tidal flow characteristics, and the wave climate (Liu et al., 1998; Liu et al., 2000). Yet the Tseng-wen River sediment discharge is found to have the greatest influence on the textural characteristics in the nearshore region off the river mouth. A major difference between the two settings, however, is in the seafloor topography seaward of the river mouth. The Tseng-wen River sediments are dispersed over a broad and shallow submarine platform of relict sediments so that the textural characteristics of the river sediments (textural signal),

including the mud portion, are widely spread over the study area. At the mouth of the Kao-ping River, however, the Kao-ping Submarine Canyon acts as a trap for the sediments, especially the mud portion. In other words, the diagnostic signal of the river sediment discharge is confined to the submarine canyon region, which in a statistical sense, is less correlated with the rest of the study area (data set). In addition, the stronger presence of mud at the seaward end of the canyon further reduces the influences of the river mud in comparison. This finding, which is only applicable within the study area, does not imply that the Kao-ping River is not an important source for sand on the Kao-ping coast. Excluding mud, the sand fraction, especially fine- to very fine-grained sand, is believed to be an important sediment source for the adjacent coast (Liu and Hou, 1997).

Both studies do share one significant finding that the northward direction is the dominant direction of sediment transport. Liu et al. (2000) have shown that the measured tidally averaged sediment flux at the mouth of Tseng-wen River is northward. In a numerical modeling study of sediment dispersal by the Tseng-wen River plume, Liu et al. (2002) discover that the river plume dynamics favors the transport of river sediment to the right-hand side (north) of the river mouth. A similar set of hydrodynamic conditions also apply to the Kao-ping River mouth. Additionally, Liu and Hou (1997) also find that northward direction is the dominant direction of longshore sediment transport off the wave-dominated Chi-jin coast. Since the Chi-jin Barrier is located in between the Kao-ping River and Tseng-wen River in southern Taiwan, the agreement suggests that on the west coast of southern Taiwan, sediments are moving predominantly in the northward direction.

7. Conclusions and future work

The Kao-ping Submarine Canyon is relatively a stratified and statically stable environment. The hydrographic characteristics of the canyon display seasonal variability controlled primarily by the

temperature field and the effluent of the Kao-ping River. The hydrographic condition and the bottom topography in the canyon suggest the propagation of internal tides during the flood season (summer) of the Kao-ping River. The submarine canyon acts as a trap and conduit for mud exchange between the Kao-ping River and offshore. Near the head of the canyon there is a region of sediment transport convergence. This region is also characterized by high mud abundance on the seafloor that coincides with the presence of high SSC spots in the bottom nepheloid layer. Outside the submarine canyon on the shelf where the evidence of wave reworking is strong, the northwestward alongshore transport dominates over the southeastward transport. There are ongoing studies to examine the relationship between the flow field inside the canyon and the flow field on the shelf, as well as to quantify the suspended sediment dynamics at the mouth of the Kao-ping River and inside the Kao-ping Submarine Canyon. We hope, through the findings of these studies, a picture of river–canyon interaction will gradually emerge.

Acknowledgements

The funding for this study was provided by the R.O.C. National Science Council under grant numbers NSC87-2611-M-110-002, and NSC88-2611-M-110-001. We are grateful for Peter Tsao's invaluable assistance in the field with the chartered boat operation. We thank Captain Wu and his crew of the R/V *Ocean Researcher III* for their assistance in the data acquisition. The courtesy of the Tung-kang Branch of the Taiwan Fisheries Research Institute to allow us to place the DGPS base station on its premises is acknowledged. We also thank Fanta Hsu for her help in the field work and sample analysis and Ray Hsu for his assistance in 3-D imaging. Kaohsiung Harbor Bureau provided the tide data, and the Water Resources Bureau provided the hydrology data of Kao-ping River. We thank an anonymous reviewer and Dr. David J.W. Piper for their helpful comments and suggestions for improving the manuscript.

References

- Baines, P.G., 1982. On internal tide generation models. *Deep-Sea Res.* 29, 307–338.
- Baker, E.T., 1976. Distribution, composition, and transport of suspended particulate matter in the vicinity of Willapa submarine canyon, Washington. *Geol. Soc. Am. Bull.* 87, 625–632.
- Baker, E.T., Hickey, B.M., 1986. Contemporary sedimentation processes in and around an active west coast submarine canyon. *Mar. Geol.* 71, 15–34.
- Carson, B., Baker, E.T., Hickey, B.M., Nittrouer, C.A., Demaster, D.J., Thorbjarnarson, K.W., Snyder, G.W., 1986. Modern sediment dispersal and accumulation in Quinault submarine canyon – a summary. *Mar. Geol.* 71, 1–13.
- Durrieu de Madron, X., 1994. Hydrography and nepheloid structures in the Grand-Rhone canyon. *Cont. Shelf Res.* 14, 457–477.
- Freeland, H.J., Denman, K.L., 1982. A topographically controlled upwelling center off southern Vancouver Island. *J. Mar. Res.* 40, 1069–1093.
- Friedrichs, C.T., Wright, L.D., 1995. Resonant internal waves and their role in transport and accumulation of fine sediment in Echernforde Bay, Baltic Sea. *Cont. Shelf Res.* 15, 1697–1721.
- Gao, S., Collins, M., 1992. Net sediment transport patterns inferred from grain-size trends, based upon definition of ‘transport vectors’. *Sediment. Geol.* 80, 47–60.
- Gao, S., Collins, M., 1994. Analysis of grain size trends, for defining sediment transport pathways in marine environments. *J. Coast. Res.* 10, 70–78.
- Gao, S., Collins, M., Lanckneus, J., Moor, G., Van Lancker, V., 1994. Grain size trends associated with net sediment transport patterns: An example from the Belgian continental shelf. *Mar. Geol.* 121, 171–185.
- Gardner, W.D., 1989. Baltimore Canyon as a modern conduit of sediment to the deep sea. *Deep-Sea Res.* 36, 323–358.
- Granata, T.C., Vidondo, B., Duarte, C.M., Satta, M.P., Gracia, M., 1999. Hydrodynamics and particles transport associated with a submarine canyon off Blanes (Spain), NW Mediterranean Sea. *Cont. Shelf Res.* 19, 1249–1263.
- Hagen, R.A., Vergara, H., Naar, D.F., 1996. Morphology of San Antonio Submarine canyon on the central Chile forearc. *Mar. Geol.* 129, 197–205.
- Hickey, B., Baker, E., Kachel, N., 1986. Suspended particle movement in and around Quinault submarine canyon. *Mar. Geol.* 71, 35–83.
- Hotchkiss, F.S., Wunsch, C., 1982. Internal waves in Hudson Canyon with possible geological implications. *Deep-Sea Res.* 29, 415–442.
- Inman, D.L., Frautschy, J.D., 1966. Littoral processes and the development of shoreline. In: *Proceedings of the Coastal Engineering Speciality Conference*, Santa Barbara, CA. American Society of Civil Engineers, Portland, OR, pp. 511–536.
- Jeng, W.-l., Wang, J., Han, B.-c., 1996. Coprostanol distribution in marine sediments off southeastern Taiwan. *Environ. Pollut.* 94, 47–52.
- Kinsella, E.D., Hay, A.E., Denner, W.W., 1987. Wind and topographic effects on the Labrador Current and Carson Canyon. *J. Geophys. Res.* 92, 10853–10869.
- Klink, J.M., 1996. Circulation near submarine canyons: A modeling study. *J. Geophys. Res.* 101, 1211–1223.
- Knauss, J.A., 1978. *Introduction to Physical Oceanography*. Prentice-Hall, Englewood Cliffs, NJ, 338 pp.
- Liu, J.T., Hou, L.-h., 1997. Sediment trapping and bypassing characteristics of a stable tidal inlet at Kaohsiung Harbor, Taiwan. *Mar. Geol.* 140, 367–390.
- Liu, J.T., Huang, J.-s., Chyan, J.-m., 2000. The coastal depositional system of a small mountainous river: a perspective from grain-size distributions. *Mar. Geol.* 165, 63–86.
- Liu, J.T., Chao, S.-Y., Hsu, R.T., 2002. Numerical modelling study of sediment dispersal by a river plume. *Continental Shelf Research*, in press.
- Liu, C.-S., Huang, I.L., Teng, L.S., 1997. Structural features off southeastern Taiwan. *Mar. Geol.* 137, 305–319.
- Liu, J.T., Yuan, P.B., Hung, J.-j., 1998. The coastal transition at the mouth of a small mountainous river in Taiwan. *Sedimentology* 45, 803–816.
- Liu, J.T., Zarillo, G.A., 1989. Distribution of grain sizes across a transgressive shoreface. *Mar. Geol.* 87, 121–136.
- Liu, J.T., Zarillo, G.A., 1990. Shoreface dynamics: evidence from sediment patterns and bathymetry. *Mar. Geol.* 94, 37–53.
- McLaren, P., 1981. An interpretation of trends in grain size measure. *J. Sediment. Petrol.* 51, 611–624.
- McLaren, P., Bowles, D., 1985. The effect of sediment transport of grain-size distributions. *J. Sediment. Petrol.* 55, 457–470.
- Ribbe, J., Holloway, P.E., 2001. A model of suspended sediment transport by internal tides. *Cont. Shelf Res.* 21, 395–422.
- Sherwin, T.J., Taylor, N.K., 1990. Numerical investigations of linear internal tide generation in the Rockall Trough. *Deep-Sea Res.* 37, 1595–1618.
- Skene, K.I., Mulder, T., Syvitski, J.P.M., 1997. INFLO1: A model predicting the behavior of turbidity currents generated at river mouths. *Comput. Geosci.* 23, 975–991.
- Wang, J., Chern, C.-s., 1996. Preliminary observations of internal surges in Tung-kang. *Acta Oceanogr. Taiwanica* 35, 17–40.
- Wang, J., Chern, C.-s., Liu, A.K., 2000. The wavelet empirical orthogonal function and its application to the analysis of internal tides. *J. Atmos. Ocean. Technol.* 17, 1403–1420.
- Water Resources Bureau, 1998. *Hydrological Year Book of Taiwan, Republic of China, 1997*. Ministry of Economic Affairs, R.O.C., 378 pp.
- Wei, C.H., Lai, T.C., Sun, C.T., Yu, K.C., Chang, K.T., Shern, J.C., Chen, M.S., 1988. An investigated study on sea state at near shore of Chi-jin coast. *National Kaohsiung Institute of Marine Technology, Rep. No. 007*, 181 pp.
- Wei, C.H., Shern, J.C., Lee, C.P., Lai, T.C., 1990. Report on

- the hydraulic model study of the Chi-jin Ocean Cultural World. National Kaohsiung Institute of Marine Technology, Rep. No. 009, 216 pp.
- Yu, H.-s., Auster, P.J., Cooper, R.A., 1993. Surface geology and biology at the head of Kao-ping canyon off southeastern Taiwan. *Terr. Atmos. Ocean. Sci.* 4, 441–455.
- Yu, H.-s., Hong, E., 1993. The Haupingsu channel/canyon system off northwestern Taiwan: Morphology, sediment character and origin. *Terr. Atmos. Ocean. Sci.* 4, 307–319.
- Yu, H.-s., Huang, C.-s., Ku, J.-w., 1991. Morphology and possible origin of the Kao-ping submarine canyon head off southeast Taiwan. *Acta Oceanogr. Taiwanica* 27, 40–50.
- Yu, H.-s., Wen, Y.-h., 1991. Morphology and echo characters of Fangliao submarine canyon off southeast Taiwan. *Acta Oceanogr. Taiwanica* 26, 1–16.